

## Article

# Reassessing Breast Cancer-Associated Fibroblasts (CAFs) Interactions with Other Stromal Components and Clinico-Pathologic Parameters by Using Immunohistochemistry and Digital Image Analysis (DIA)

Alina Cristina Barb<sup>1,2,3</sup>, Mihaela Pasca Fenesan<sup>1,2,3</sup>, Marilena Pirtea<sup>1</sup>, Mădălin-Marius Margan<sup>4</sup> , Larisa Tomescu<sup>2,5</sup> , Emil Ceban<sup>6,7</sup>, Anca Maria Cimpean<sup>1,8,\*</sup>  and Eugen Melnic<sup>9</sup>

- <sup>1</sup> Department of Microscopic Morphology/Histology, Victor Babes University of Medicine and Pharmacy, 300041 Timisoara, Romania; toma.alina@umft.ro (A.C.B.); fenesan.mihaela@gmail.com (M.P.F.); pirtea.laurentiu@umft.ro (M.P.)
- <sup>2</sup> Doctoral School in Medicine, Victor Babes University of Medicine and Pharmacy, 300041 Timisoara, Romania; tomescu.larisa@umft.ro
- <sup>3</sup> Department of Clinical Oncology, OncoHelp Hospital, 300239 Timisoara, Romania
- <sup>4</sup> Department of Functional Sciences/Discipline of Public Health, Victor Babes University of Medicine and Pharmacy, 300041 Timisoara, Romania; marganmm@gmail.com
- <sup>5</sup> Department of Obstetrics and Gynecology, "Victor Babes" University of Medicine and Pharmacy Timisoara, 300041 Timisoara, Romania
- <sup>6</sup> Department of Urology and Surgical Nephrology, Nicolae Testemitanu State University of Medicine and Pharmacy, 2004 Chisinau, Moldova; emil.ceban@usmf.md
- <sup>7</sup> Laboratory of Andrology, Functional Urology and Sexual Medicine, Nicolae Testemitanu State University of Medicine and Pharmacy, 2004 Chisinau, Moldova
- <sup>8</sup> Center of Expertise for Rare Vascular Disease in Children, Emergency Hospital for Children Louis Turcanu, 300011 Timisoara, Romania
- <sup>9</sup> Department of Pathology, Nicolae Testemitanu State University of Medicine and Pharmacy, 2004 Chisinau, Moldova; eugen.melnic@usmf.md
- \* Correspondence: acimpeanu@umft.ro; Tel.: +40-720-060-955



**Citation:** Barb, A.C.; Fenesan, M.P.; Pirtea, M.; Margan, M.-M.; Tomescu, L.; Ceban, E.; Cimpean, A.M.; Melnic, E. Reassessing Breast Cancer-Associated Fibroblasts (CAFs) Interactions with Other Stromal Components and Clinico-Pathologic Parameters by Using Immunohistochemistry and Digital Image Analysis (DIA). *Cancers* **2023**, *15*, 3823. <https://doi.org/10.3390/cancers15153823>

Academic Editor: David Wong

Received: 22 June 2023

Revised: 18 July 2023

Accepted: 25 July 2023

Published: 27 July 2023



**Copyright:** © 2023 by the authors. Licensee MDPI, Basel, Switzerland. This article is an open access article distributed under the terms and conditions of the Creative Commons Attribution (CC BY) license (<https://creativecommons.org/licenses/by/4.0/>).

**Simple Summary:** Breast cancer (BC) is primarily classified by immunohistochemistry (IHC) and digital image analysis (DIA) based on distinct immunophenotypes of malignant epithelial cells. When antiangiogenic and immunomodulatory therapies are used for BC, the stromal components such as tumor vessels and immune cells have received more attention. Cancer-associated fibroblasts (CAFs) are extensively investigated, but measuring them in immunostained tissues and determining how they relate to clinical and pathological criteria is still difficult in BC. Our earlier research using CD34 and  $\alpha$ -smooth muscle actin ( $\alpha$ SMA) immunohistochemistry showed a decrease of CD34-positive CAFs and an increase of  $\alpha$ SMA-positive CAFs inside the tumor stroma. This early basic microscopic finding gives us the intention to employ DIA to improve SMA-positive CAF quantification accuracy. Additional DIA processed data correlations to pathologic parameters, survival, invasion, and recurrence indicated substantial differences between BC molecular subtypes, suggesting a unique CD34- and  $\alpha$ SMA-positive CAF impact for each subtype.

**Abstract:** Background: Breast cancer (BC) stroma has CD34- and  $\alpha$ SMA-positive cancer-associated fibroblasts (CAFs) differently distributed. During malignant transformation, CD34-positive fibroblasts decrease while  $\alpha$ SMA-positive CAFs increase. The prevalence of  $\alpha$ SMA-positive CAFs in BC stroma makes microscopic examination difficult without digital image analysis processing (DIA). DIA was used to compare CD34- and  $\alpha$ SMA-positive CAFs among breast cancer molecular subgroups. DIA-derived data were linked to age, survival, tumor stroma vessels, tertiary lymphoid structures (TLS), invasion, and recurrence. Methods: Double immunostaining for CD34 and  $\alpha$ SMA showed different CAF distribution patterns in normal and BC tissues. Single CD34 immunohistochemistry on supplemental slides quantified tumor stroma CD34\_CAFs. Digital image analysis (DIA) data on CAF density, intensity, stromal score, and H-score were correlated with clinico-pathologic factors. Results:

CD34/ $\alpha$ SMA CAF proportion was significantly related to age in Luminal A (LA), Luminal B (LB), and HER2 subtypes. CD34\_CAF influence on survival, invasion, and recurrence of LA, LB-HER2, and TNBC subtypes was found to be significant. The CD34/ $\alpha$ SMA-expressing CAFs exhibited a heterogeneous impact on stromal vasculature and TLS. Conclusion: BC stromal CD34\_CAFs/ $\alpha$ SMA\_CAFs have an impact on survival, invasion, and recurrence differently between BC molecular subtypes. The tumor stroma DIA assessment may have predictive potential to prognosis and long-term follow-up of patients with breast cancer.

**Keywords:** cancer-associated fibroblasts (CAFs); CD34\_CAFs;  $\alpha$ SMA\_CAFs; immunohistochemistry (IHC); digital image analysis (DIA); breast cancer (BC); tumor stroma

## 1. Introduction

Cancer-associated fibroblasts (CAFs) represent a significant constituent of the tumor microenvironment in cases of breast cancer (BC). Prior research has demonstrated that these entities are notably diverse and intimately linked with tumor cells and other stromal constituents, such as tumor stroma vessels or immune cells. However, the precise mechanisms underlying these intricate interactions remain incompletely understood [1,2]. Various CAF markers have been employed to categorize CAFs in breast cancer into distinct subgroups, potentially exerting a unique influence on molecular subtypes of breast cancer. Despite the heterogeneity of markers for cancer-associated fibroblasts (CAFs), there is currently no specific marker that can accurately define each type of CAF. Ongoing efforts are being made to identify additional markers for this purpose [1,3]. Research on the tumor microenvironment's cancer-associated fibroblasts (CAFs) has extended beyond the stroma of primary cancers. In recent publications, there has been a presentation of data on the heterogeneity of CAFs from the stroma of metastases [4,5]. Vimentin, fibroblast-associated protein (FAP), CD34, and alpha smooth muscle actin ( $\alpha$ SMA) are the most frequently utilized markers for evaluating cancer-associated fibroblasts (CAFs). Divergent expression of CD34-positive fibroblasts in breast normal tissue and alpha smooth muscle actin ( $\alpha$ SMA) cancer-associated fibroblasts (CAFs) inside breast cancer (BC) stromal compartment is not a new topic in the field [6–10], but its prognostic and therapeutic impact is still controversial [8,11] and incompletely understood [12–15]. Most of these studies were performed on classical BC histopathology, and few of them assessed CD34 fibroblasts and  $\alpha$ SMA\_CAFs related to different molecular subtypes. Despite the recently reported complex heterogeneity markers expressed by CAFs [16], CAFs' prognostic and therapeutic role is extremely limited [16,17]. Most of the studies focused on CD34/ $\alpha$ SMA\_CAF interplay in BC stroma used manual semiquantitative methods to assess immunohistochemical staining and to classify them as “present” or “absent”. Also, the stratification of immunostaining intensity is highly influenced by different perceptions of people who assessed BC specimens by conventional microscopic methods. This is a very limited subjective method related to the lack of its ability to count positive cell density (especially for  $\alpha$ SMA-positive cells which are present in a high amount inside tumor stroma and, moreover, are closely packed or form networks, thus being impossible to count) [18–21]. On the other side, the CD34-positive fibroblasts dramatically decrease from normal breast stroma to tumor stroma, and they are wrongly considered to be absent inside stromal compartment surrounding malignant areas [6,18]. This basic interpretation seems to be the main reason why there are scattered correlative data in between CD34\_CAFs and prognostic factors in BC. CD34-positive stromal cells are usually named stromal telocytes and are reported to be stromal progenitor cells with a high ability to differentiate into other stromal cells including  $\alpha$ SMA-positive myofibroblasts during tissue repair, regeneration, inflammatory processes, or malignancies [22–27]. A pathologist who evaluates a BC tissue slide is highly tempted to be focused on tumor cells rather than cellular and vascular stromal components. A routine IHC antibody panel for BC evaluation does not usually include CD34 and  $\alpha$ SMA due to the lack of their expression

in tumor cells. CD34 may be used as marker for tumor blood vessels when the pathologist needs vascular invasion confirmation [28].  $\alpha$ SMA immunostaining is used during routine histopathologic diagnosis as a marker for myoepithelial cells and is helpful to evaluate controversies related to microinvasion or for papillary and spindle cells lesions [28]. At this time, BC stroma assessment is not included by pathologists in routine diagnostic evaluation of BC patients, and it has no certified predictive or prognostic role in routine microscopic evaluation despite the recent data which mentioned BC tumor stroma as a potential target for innovative therapies [29,30]. Currently, there are no established guidelines on how to process and evaluate BC stroma CD34 and  $\alpha$ SMA CAFs, most likely due to the lack of proper tools to accomplish this. The tumor–stroma ratio proved itself to be a predictor and have a prognostic impact on BC based upon the results of retrospective studies performed on human BC specimens [31–33]. For tumor–stroma ratio evaluation, there are already well-developed and standardized digital tools for automated assessment [34,35]. The ability of the human eye to evaluate histology slides is limited. Hence, computer-aided quantitative digital image analysis (DIA) offers a more thorough evaluation of many components [36–39]. However, due to its time-consuming nature and limited accessibility, this technique is not frequently employed. Lumongga et al. [40] assessed vimentin positive tumor stroma fibroblasts by their intensity but not by their density using Image J as a digital image analysis tool, and this assessment was limited to triple negative breast cancer molecular subtype [40].

The investigation of CAFs has been the subject of extensive research. However, the measurement of CAFs in immunostained tissues and the determination of their relationship with clinical and pathological criteria remain challenging in the context of breast cancer. Our previous investigations utilizing CD34 and  $\alpha$ -smooth muscle actin ( $\alpha$ SMA) immunohistochemistry revealed a reduction in CD34-positive cancer-associated fibroblasts (CAFs) and a rise in  $\alpha$ SMA-positive CAFs within the tumor stroma [6]. This preliminary microscopic observation leads us to the aim of this present study to use digital image analysis (DIA) to enhance the precision of quantifying smooth muscle actin (SMA)-positive cancer-associated fibroblasts (CAFs). The analysis of further processed data by DIA could reveal significant variations among the molecular subtypes of breast cancer in terms of pathologic parameters, survival, invasion, and recurrence. Based on all these previous data, we hypothesized that the impact of CD34- and  $\alpha$ SMA-positive cancer-associated fibroblasts (CAFs) may be distinct for each subtype and may be accurately enhanced by using DIA associated with immunohistochemistry interpretation.

We propose here the quantification of CD34 and  $\alpha$ SMA tumor stromal CAFs by using a stromal score (SS) which combines both intensity and density of stromal positive cells and H-score automatically generated by QuPath digital image analysis software. Density and intensity of positive stromal cells together with SS and H-score will be interpreted related to their impact on age, survival rate, BC molecular subtype, vascular and immune stromal components, invasion, and recurrence.

## 2. Materials and Methods

### 2.1. The Selection of Patients and Ethical Considerations

The present investigation is a part of a larger retrospective study that includes 150 breast cancer formalin-fixed paraffin-embedded (FFPE) specimens obtained from women with ductal invasive carcinoma on histopathology identified between 2015 and 2022 and ranging in age from 32 to 85 years old. Two different pathologists performed a second round of analysis on the FFPE tissues to confirm the diagnosis and select cases for immunohistochemistry. A molecular profile was determined for each individual case using immunohistochemistry markers. These markers included the Estrogen Receptor (ER), the Progesterone Receptor (PR), the Proliferation Index (Ki67), and an evaluation for the Human Epidermal Growth Factor Receptor 2 (HER2). This was necessary to determine the different breast cancer molecular subtypes. For the goal of this investigation, we chose 53 patients who possessed a complete clinical, histopathological, and therapeutic profile

that would be helpful for our purposes. Age, menopausal status, breast cancer molecular subtype, tumor grade (G), Nottingham Prognostic Index (NPI), lymphovascular invasion, perineurial invasion, and recurrence were chosen as the clinicopathologic and therapeutic factors for this study. From stromal components, we selected tertiary lymphoid structures (TLS, previously assessed on the same cases) and immature (CD34+/ $\alpha$ SMA-) or mature (CD34+/ $\alpha$ SMA+) stromal tumor blood vessels to be correlated with stromal CAFs. At the time of the diagnosis, none of the patients had a previous history of metastases that could be confirmed by imaging techniques. Based on a standardized form that had previously been reviewed and approved by the Research Ethics Council of the “Victor Babeș” University of Medicine and Pharmacy in Timișoara (No. 49/28.09.2018), informed permission was obtained from each patient.

### *2.2. Initial Processing, Histology, and Selection of Formalin-Fixed Paraffin-Embedded (FFPE) Specimens for Immunohistochemistry*

Briefly, pieces of the tumor were obtained for the initial diagnosis before any treatment was administered using a combination of mastectomy and needle core biopsy. A piece of the tumor and the area surrounding the tumor that was indicative of the whole were chosen. After obtaining breast cancer tissue samples and storing them in buffered formalin for 24 to 48 h, the specimens were then embedded in paraffin according to the conventional method. Each FFPE block was sectioned to a thickness of three micrometers, and the resulting sections were put on glass slides. In order to do a histopathologic examination, one slide was taken from each case and stained with hematoxylin and eosin. Two separate pathologists evaluated the hematoxylin and eosin-stained slides that were pertinent to validate the initial histopathological diagnosis and evaluate the tissue quality. This was important to make the appropriate case selection for immunohistochemistry. The TLS was detected and quantified by the pathologists, and this was accomplished in conjunction with the histopathologic diagnosis. Vimentin immunostaining was utilized as a means of determining the overall tissue quality (clone V9). Cases with a positive vimentin staining in the tumor stroma were regarded suitable for selection and for subsequent immunohistochemical studies.

### *2.3. Immunohistochemistry*

Immunohistochemistry (IHC) was carried out on sections that were three micrometers in thickness utilizing an autostainer manufactured by Leica Biosystems (Newcastle upon Tyne, UK). The Novocastra Bond Epitope Retrieval Solution 1 and 2 together were utilized in the process of unmasking (Leica Biosystems, Newcastle Ltd., Newcastle Upon Tyne, UK). Hydrogen peroxide at a concentration of 3% was used to inhibit endogenous peroxidase activity for a period of five minutes. A method using double immunostaining was carried out on some tissue specimens in order to conduct the interplay in between CD34-positive fibroblasts known to be common for normal breast tissue stroma and SMA\_CAFs highly present inside the stromal component of BC tissue. A differentiated analysis of mature and immature tumor blood vessels originating from the BC stromal component was also performed and analyzed previously, and data were correlated to CAFs parameters. We used CD34 mouse anti-human monoclonal antibodies (clone, QBEnd 10, Leica Biosystems, Newcastle upon Tyne, UK, 30 min incubation time at room temperature) for the endothelium of tumor blood vessels and fibroblasts from normal and tumor stroma. Additionally, we used alpha smooth muscle actin (SMA) mouse anti-human monoclonal antibodies (clone 1A4, Leica Biosystems, Newcastle upon Tyne, UK, 30 min incubation time at room temperature) for perivascular cells and CAFs from the tumor stroma. The completion of the immunohistochemical method required the use of visualization systems such as the Bond Polymer Refine Detection System DAB and the Bond Polymer Refine Red Detection System. On additional slides from each case, we performed immunohistochemistry for CD34 as single marker in order to help us form an accurate assessment of CD34\_CAFs. Slides that had been stained with immunohistochemistry were mounted with a permanent mounting

medium called CV Mount, which was manufactured by Leica Biosystems, New-castle Ltd., in the United Kingdom.

#### 2.4. Image Acquisition and Digital Image Analysis (DIA)

IHC samples were scanned using a Grundium OCUS 20 Microscope (Grundium, Tampere, Finland) and stored in the Case Center Slide Library as svf files (3DHistech, Budapest, Hungary). A project has been created by importing all slides stained with CD34/SMA and CD34 alone into QuPath version 0.4.3 [41], an open-source platform for bioimage analysis of microscopic slides, where they were examined using integrated software and its add-ons, such as Fiji and Vascular Analysis, for an accurate evaluation of tumor stromal blood vessels. Usually, QuPath was used in the literature to assess tumor stroma ratio which seems to have a significant prognostic impact [42]. Briefly, we selected 3–5 regions of interests (ROIs) (Figure 1A) from tumor stroma by using the brush tool which gave us the most accurate delineation of tumor stroma from tumor tissue and also excluded stromal blood vessels (assessed by QuPath/Vessels analysis, previously). DIA started with a pre-processing step consisting of estimating stain vectors (Figure 1B). Then, the analysis continued with cell detection by choosing a positive cell detection option and by setting cell parameters and intensity parameters. The detection image was set for an optical density sum with a requested pixel size of 0.5  $\mu\text{m}$  and a cell expansion of 1.988  $\mu\text{m}$ , excluding the nucleus. Intensity threshold parameters comprised the score compartment and three threshold levels evaluated as weak (+1, highlighted with yellow), moderate (+2, highlighted with orange), and high (+3, highlighted in red), with all cells selected in blue being considered negative (Figure 1C,D). During automated scoring, QuPath software provided us the cell count, percentage of positive and negative stromal cells, both density score and intensity score separately, but also a combined Stromal Score (SS, similar to the Allred score, combining intensity and density of positive detected stromal CAFs). Also, an H-score was included in the final evaluation conducted by QuPath analysis (Figure 1E). For our study, we used positive stromal CAF intensity (S\_SMA\_I and S\_CD34\_I, respectively), density (S\_SMA\_D and S\_CD34\_D, respectively), SS (CD34\_SS and SMA\_SS), and H-score (CD34\_H-Score and SMA\_H-Score) for a more accurate evaluation and correlation with clinic-pathologic parameters.

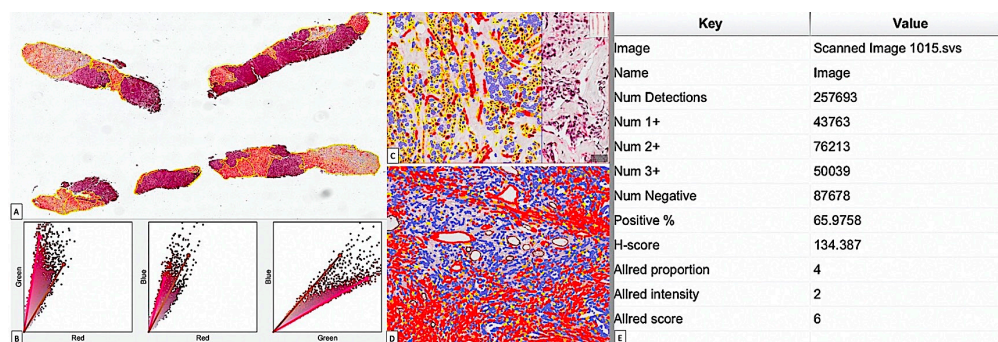


**Figure 1.** Digital image analysis (DIA) of CAFs using the QuPath open-source platform for bioimage analysis. (A) Regions of interest (ROIs) were chosen by using brush tool from QuPath tools. Stroma areas were sharply delineated by the tumor areas. (B) Vector stain estimation followed during DIA evaluation, and a visual stain map was generated. (C,D) Stromal CAFs were counted separately according to the cell parameters and intensity score set by the user. Note that three intensity thresholds (weak-yellow, noted as +1; intermediate-orange, noted as +2; and high-red, noted as +3) were used, and cells with different intensity were reported separately. Stromal and/ or tumor cells detected as negative were highlighted in blue by QuPath\_DIA. (E) Example of a report table regarding the parameters automatically delivered by QuPath analysis. Allred score from the final report was considered by us as a Stromal Score including both proportion and intensity of total number of cells counted inside selected stromal areas.

### 2.5. Statistical Analysis

JAMOVI software version 2.3 for macOS devices was used for statistical analysis. DIA-derived data mentioned above were correlated with BC molecular subtypes, menopausal status, immature and mature stromal blood vessels, recurrence, lymphovascular and perineural invasion, and age. A statistical correlation was assessed and considered significant for a  $p$  value of 0.05 or less.

## 3. Results

### 3.1. General Considerations on Conventional Microscopic Assessment of Stromal CD34 and $\alpha$ SMA in Normal Breast Tissue and BC

A divergent expression of CD34 and  $\alpha$ SMA has been observed in the present study. Single IHC for CD34 revealed that positive cell density dramatically decreased from normal to malignant tissue (Figure 2A), remaining positive in tumor vessels' endothelium and a few CAFs in scattered areas in between tumor cells (Figure 2B). Double IHC for CD34 and  $\alpha$ SMA identified high CD34 expression in the stroma surrounding the Terminal Ductal Lobular Unit (TDLU) of the normal breast (Figure 2C).  $\alpha$ SMA positivity was found to be restricted to myoepithelial cells from the ductal and lobular structure of a normal mammary gland (Figure 2D) while the inside tumor stroma predominated  $\alpha$ SMA-positive CAFs with a high density and staining intensity (Figure 2E). Rare cases presented an intermixed area of  $\alpha$ SMA positive CAFs (predominant) and CD34-positive CAFs (scattered) (Figure 2F).

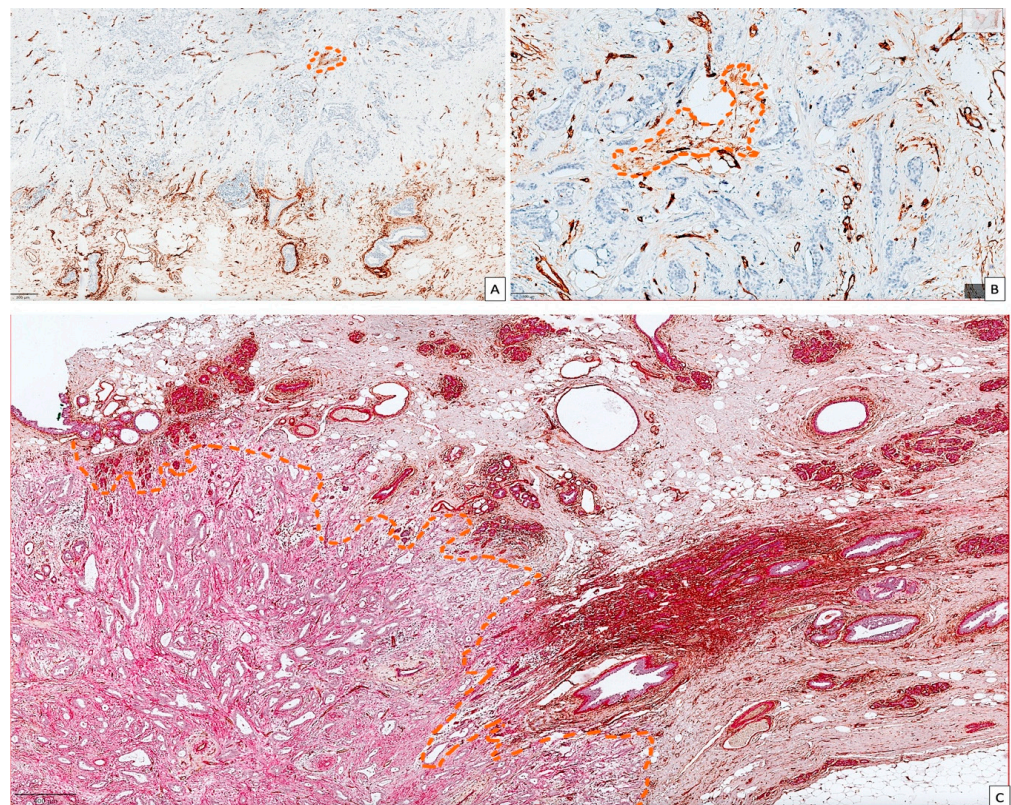
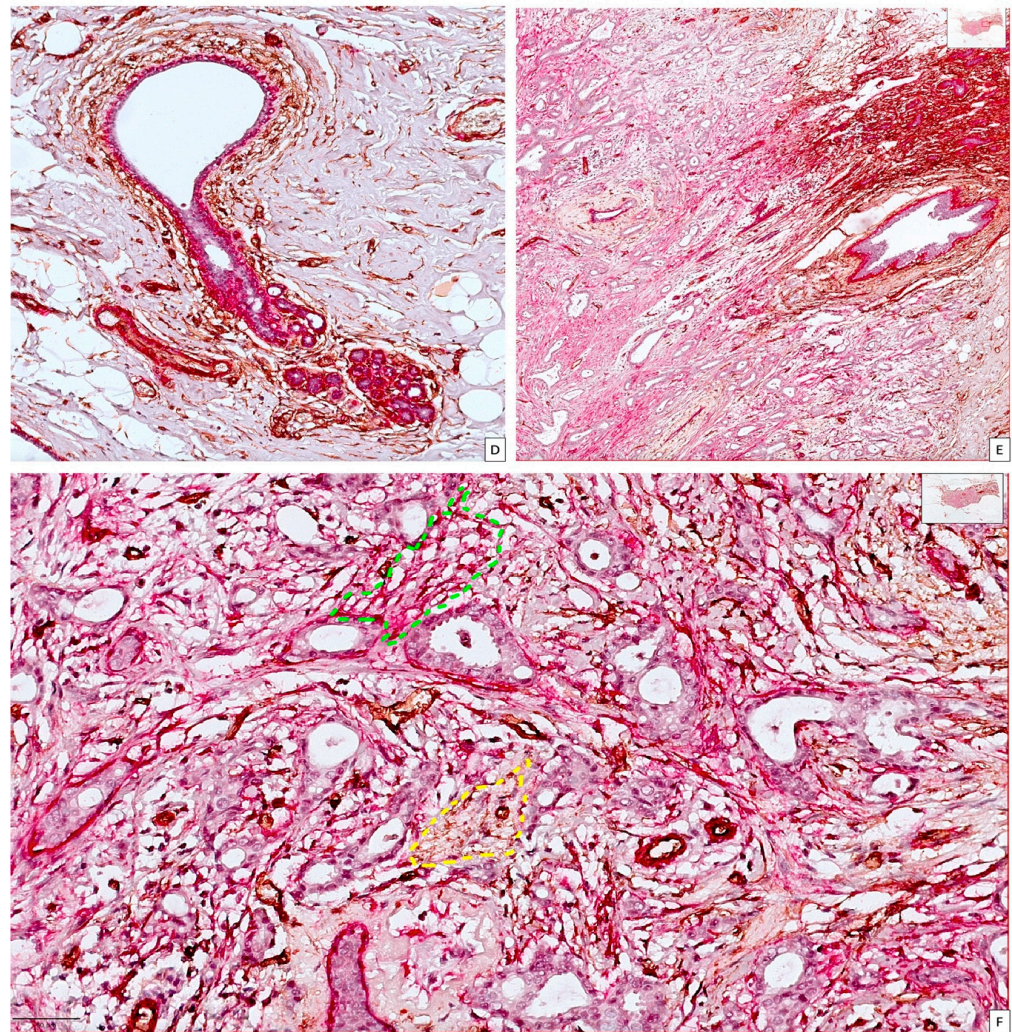


Figure 2. Cont.



**Figure 2.** CD34 single (A,B) and double CD34/ $\alpha$ SMA (C–F) immunohistochemical stains for BC tissues included in our study for highlighting CAFs and normal stromal fibroblast plasticity. (A) CD34-positive fibroblast density dramatically decreased from normal (low part of the picture) to malignant tissue (upper part of the picture) but did not completely disappear, being restricted to small intratumor areas (dotted orange line). (B) Deep inside BC tissue, small foci of CD34-positive CAFs were detected (dotted orange limited area), but mostly, CD34 positivity was observed inside the tumor blood vessels endothelium. (C) CD34/ $\alpha$ SMA double-stain (CD34—brown and  $\alpha$ SMA—red) sharply delineated differences in between CD34 and  $\alpha$ SMA expression in between normal breast tissue (right to the orange dotted line) and BC tissue (left to the dotted line). (D) Normal TDLU expressing  $\alpha$ SMA restricted to myoepithelial cells which delineate both ductal and acinar components, while CD34 is highly expressed in peri-TDLU stromal fibroblasts but also fibrocytes from dense interlobular stroma. (E) Border in between normal and tumor tissue highlighted by the change in the density and intensity of  $\alpha$ SMA expression. (F) Detail from BC area with a high predominance of  $\alpha$ SMA\_CAFs (red) inside stroma (multiple areas similar with green dotted lined area) and small and inconstant foci of CD34\_CAFs (yellow dotted lined area). Because of these scattered CD34-positive intratumor CAFs, both immunostains were mandatory for a more accurate CAFs heterogeneity evaluation.

### 3.2. Critical Overview of Digital Image Analysis for BC Stromal CAF Assessment by Using Immunohistochemistry and QuPath Platform

#### 3.2.1. $\alpha$ SMA\_CAF Digital Image Analysis

We performed both single (for CD34) and double (CD34/ $\alpha$ SMA) immunohistochemistry for identification of both CD34\_CAFs and  $\alpha$ SMA\_CAFs. CD34/ $\alpha$ SMA double-staining was performed to identify stromal immature and mature blood vessels and for quantifi-

cation of  $\alpha$ SMA\_CAFs. It is well known that the manual evaluation of both CD34- or  $\alpha$ SMA-positive CAFs is practically impossible due usually to a low density (for CD34) and too many high-density (for  $\alpha$ SMA) CAFs from the BC stromal compartment. For these cases, the usual interpretation performed manually on IHC slides includes a subjective microscopic appreciation of both CAF density and intensity based on empirical criteria chosen by each pathologist. For example, for cell density three scores are often used: low—often noted as 10–30 positive cells, medium—noted as 30–60 positive cells, and high—noted as 60–100 positive cells on randomly selected BC stroma areas. By applying this algorithm, it seems that cases from Figure 3A,B should be categorized as having low expression for  $\alpha$ SMA\_CAFs, cases from Figure 3C,D should be categorized as having medium expression, and those from Figure 3E should be categorized as having high expression, undoubtedly. By using the QuPath bioimage analysis platform facilities, we were able to stratify cases into three classes (by giving a density scoring from 3 to 5, based on  $\alpha$ SMA\_CAF density automatically marked as it has been shown in Figure 3F–J by QuPath software according to cell parameters settings). Also, QuPath has an assessing option of staining intensity by marking cell borders (Figure 3F–J) or cell borders and their cytoplasmic area (Figure 3K–O) with different colored lines specific for each intensity varying from 1 (considering as weak, marked in yellow) to 2 (medium intensity corresponding to an orange line) and 3 (quantified as strong by a red line around positive cells). Cells marked in blue were classified as negative for immunostaining. The final score named by us as Stromal Score (SS) was calculated similar to the Allred score (with a chosen option of not counting nuclei, just cytoplasmic immunoreaction) by the sum of intensity and density for each case and varied from 4 to 8 in the present study (Figure 3A–O). An additional H-Score based on intensity pixel assessment was added as a parameter and varied from 41.366 to 276.149 for  $\alpha$ SMA\_CAFs. Automated evaluation of  $\alpha$ SMA\_CAFs revealed different densities and intensities in between BC molecular subtypes.

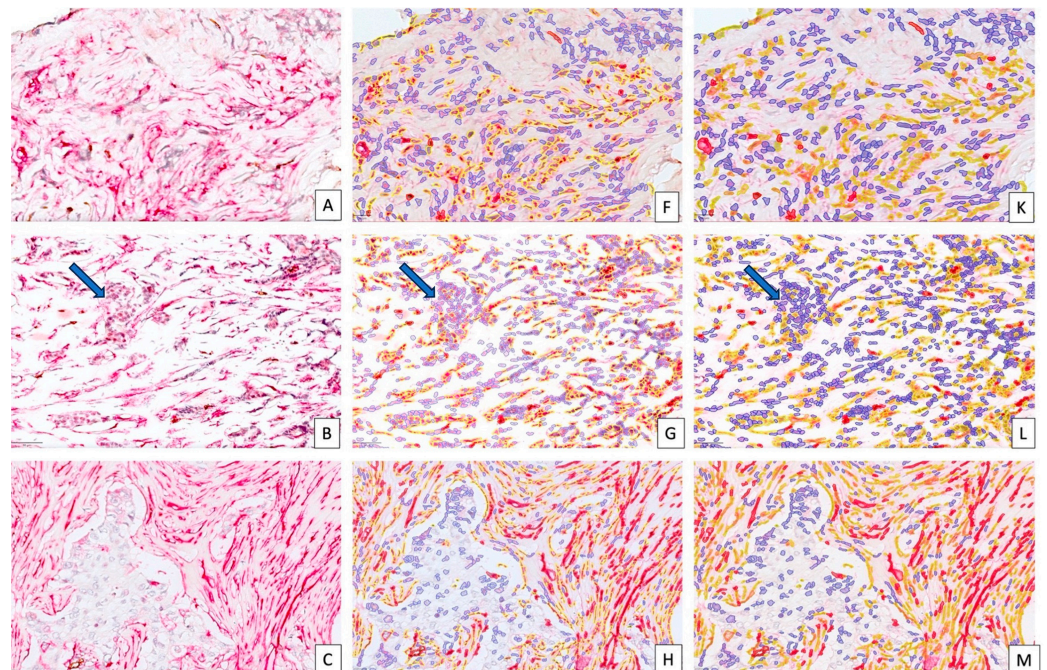
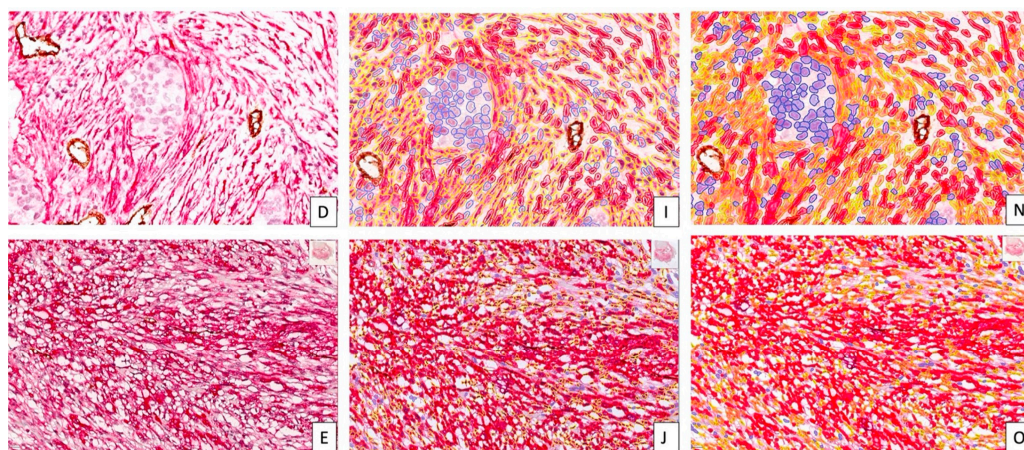


Figure 3. Cont.



**Figure 3.** Examples of  $\alpha$ SMA Stromal Scores from score 4 (A,F,K), to maximal score 8 (E,J,O). Double-stain CD34/ $\alpha$ SMA (DAB, brown/permanent red, red) was highlighted from (A–E). Stromal  $\alpha$ SMA were automatically labeled based on cell and intensity parameter settings in a different manner according to variable intensity (blue—negative, yellow—weak, +1, orange—medium, +2 and red—strong, +3). The method accuracy is high because QuPath analysis may detect tumor-infiltrating cells in the stroma, in between  $\alpha$ SMA\_CAFs, and label them as negative ((B,G,L), corresponding to a case scored as 5). Groups of infiltrating tumor cells ((B), arrow) marked to be negative by automated analysis ((G,L), arrows). When we compared images (C,D) by conventional analysis, we were tempted to consider them as having a similar density and intensity of  $\alpha$ SMA\_CAFs. But this subjective observation was not confirmed by DIA which helped us to classify cases in two different scoring groups based on proportion of different kind of positive cells (H,I). DIA detected differences between the proportion of weak, moderate, and strong positive cells, and this was extremely important for the final stromal score (M–O) impossible to differentiate by using conventional assessment). When we compared picture (F) with (G), we observed differences between the proportions of yellow-, blue-, and red-labeled cells. In (F), blue- and yellow-labeled cells predominated while for (G), red-labeled cells' proportion slightly increased together with the yellow-labeled proportion (according to automated measurements given by QuPath analysis). This fact was confirmed better by images (K,L). The Stromal Score increases once the proportion of red-labeled cells increases ((H) with an SS of 6, (I) with an SS of 7, and (J) with an SS of 8). By using the brush tool from the QuPath menu, we were able to identify CD34-positive vessels from the tumor stroma and exclude them from quantification (I,N).

### 3.2.2. CD34\_CAF Image Analysis

CD34\_CAF image analysis performed with QuPath revealed that, despite their extremely low density inside tumor stroma, they may quantify and have a clinical and prognostic impact specific for some BC molecular subtypes. Due to their low number in tumor stroma tissue, it is hard to estimate them on the same slide by a double immunostaining with  $\alpha$ SMA because of the high number and intensity staining of  $\alpha$ SMA\_CAFs which would mask CD34\_CAFs.

Thus, we evaluated CD34\_CAFs separately on a CD34 simple immunostained specimen. CD34\_CAF DIA parameters were lower compared to similar ones for  $\alpha$ SMA\_CAFs. CD34\_CAF density ranged between 2 and 4, with none of the cases reaching a density score of 5. Amongst them, 58.5% were scored as 2 for density; 37.7% had a score of 3; and resting ones had a score of 4. A percentage of 88.7% of cases had an intensity score of 2. CD34\_SS ranged between 3 (Figure 4A–D) and 6 (Figure 4E–H), with 94.33% of cases having a CD34\_SS of 4 and 5 (56.6% of scores with 4 and 37.73% of scores with 5), with the resting ones being scored as 6. The differential impact of these stromal scores was separately evaluated in the relationship with clinic-pathologic parameters in the next section of this paper.

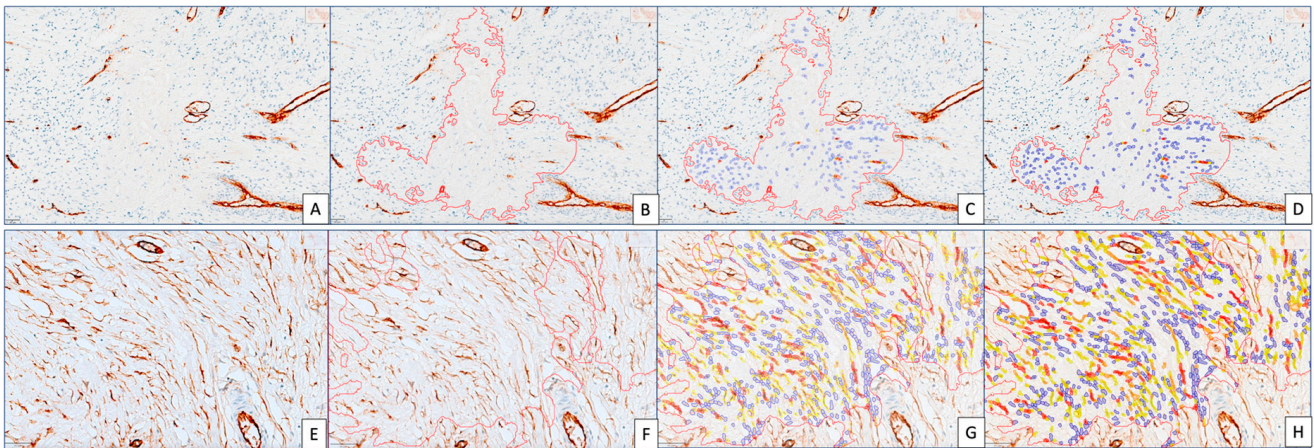


**Figure 4.** Step by step example of CD34\_CAF evaluation in BC tumor stroma by using the same digital analysis method as for  $\alpha$ SMA\_CAFs. We showed here a case scored as 3 (lowest for CD34\_CAFs, (A–D)) and a case scored as 6 (highest one for CD34\_CAFs, (E–H)).

### 3.3. DIA Impact on Stromal CD34/ $\alpha$ SMA\_CAF Assessment Related to BC Molecular Subtypes and Clinic-Pathologic Data

We performed a separate analysis for each BC molecular subtype by correlating parameters obtained from DIA to clinico-pathologic data of patients included in the study as age, menopausal status, survival, TLS, stromal vascular components, invasion, and recurrence.

#### 3.3.1. CD34/ $\alpha$ SMA\_CAF Interplay Is Highly Dependent on Age and Strongly Influences Survival and Stromal Components in Luminal A (LA\_BC) Subtype

Stromal CD34\_CAF density (S\_CD34\_D) significantly decreased for the LA stromal compartment whereas  $\alpha$ SMA\_CAF density (S\_SMA\_D) increased during malignant transformation ( $p = 0.049$ ). It seems that LA subtype is able to acquire a high number of  $\alpha$ SMA\_CAFs which in turn significantly influenced the decrease of both CD34\_SS ( $p = 0.044$ ) and CD34\_H-Score ( $p = 0.032$ ), most likely due to a low S\_CD34\_D. Patients' age had a significant impact on the  $\alpha$ SMA\_SS, being inversely but significantly correlated with it ( $p = 0.014$ ) but not with S\_SMA\_D ( $p = 0.818$ ) or SMA\_H-Score ( $p = 0.553$ ). This finding suggested that intensity and less density are influenced by age. Also,  $\alpha$ SMA\_SS had a direct significant influence on the TLS presence in the tumor stroma from LA\_BC subtype ( $p = 0.018$ ). But one of the most interesting findings related to the LA\_BC subtype was the direct significant correlation of S\_CD34\_D ( $p = 0.013$ ) and CD34\_H-Score ( $p = 0.022$ ). A low survival rate was correlated with low S\_CD34\_D for LA\_BC. No positive or negative influence on invasion and recurrence has been registered for LA\_BC in our study. All data can be summarized by the correlation matrix in Table 1.

**Table 1.** Correlation matrix for LA BC showing significant correlations for this BC molecular subtype.

		S_SMA_I	S_SMA_D	SMA_STROMAL SCORE	SMA_H-SCORE	S_CD34_I	S_CD34_D
SMA_STROMAL SCORE	Pearson's r	0.693 *	0.189	—			
	<i>p</i> -value	0.038	0.626	—			
	95% CI Upper	0.929	0.758	—			
	95% CI Lower	0.054	−0.543	—			
	Spearman's rho	0.709 *	0.189	—			
	<i>p</i> -value	0.032	0.626	—			
	Kendall's Tau B	0.685 *	0.189	—			
	<i>p</i> -value	0.045	0.593	—			
SMA_H-SCORE	Pearson's r	−0.079	0.000	−0.095	—		
	<i>p</i> -value	0.839	1.000	0.808	—		
	95% CI Upper	0.617	0.664	0.607	—		
	95% CI Lower	−0.706	−0.664	−0.714	—		
	Spearman's rho	0.040	0.000	0	—		
	<i>p</i> -value	0.919	1.000	1	—		
	Kendall's Tau B	0.075	0.000	0	—		
	<i>p</i> -value	0.801	1.000	1.000	—		
S_CD34_I	Pearson's r	−0.105	−0.286	−0.378	−0.113	—	
	<i>p</i> -value	0.788	0.456	0.316	0.772	—	
	95% CI Upper	0.601	0.467	0.382	0.596	—	
	95% CI Lower	−0.719	−0.798	−0.833	−0.723	—	
	Spearman's rho	−0.124	−0.286	−0.378	0.000	—	
	<i>p</i> -value	0.751	0.456	0.316	1.000	—	
	Kendall's Tau B	−0.120	−0.286	−0.378	0.000	—	
	<i>p</i> -value	0.726	0.419	0.285	1.000	—	
S_CD34_D	Pearson's r	0.490	−0.668 *	0.000	0.363	0.134	—
	<i>p</i> -value	0.180	0.049	1.000	0.337	0.732	—
	95% CI Upper	0.871	−0.007	0.664	0.828	0.733	—
	95% CI Lower	−0.258	−0.923	−0.664	−0.397	−0.582	—
	Spearman's rho	0.551	−0.624	0.100	0.329	0.113	—
	<i>p</i> -value	0.124	0.073	0.798	0.388	0.771	—
	Kendall's Tau B	0.502	−0.600	0.096	0.272	0.109	—
	<i>p</i> -value	0.127	0.078	0.777	0.355	0.748	—

Table 1. Cont.

		S_SMA_I	S_SMA_D	SMA_STROMAL SCORE	SMA_H-SCORE	S_CD34_I	S_CD34_D
CD34_STROMAL SCORE	Pearson's r	0.341	−0.679 *	−0.189	0.234	0.607	0.869 **
	<i>p</i> -value	0.370	0.044	0.626	0.544	0.083	0.002
	95% CI Upper	0.819	−0.026	0.543	0.778	0.906	0.972
	95% CI Lower	−0.418	−0.926	−0.758	−0.509	−0.095	0.483
	Spearman's rho	0.403	−0.661	−0.097	0.301	0.606	0.855 **
	<i>p</i> -value	0.283	0.053	0.804	0.430	0.084	0.003
	Kendall's Tau B	0.344	−0.617	−0.091	0.225	0.566	0.825 **
	<i>p</i> -value	0.281	0.062	0.784	0.433	0.087	0.01
CD34_H-SCORE	Pearson's r	0.328	−0.711 *	−0.233	0.449	0.252	0.948 ***
	<i>p</i> -value	0.389	0.032	0.546	0.225	0.514	<0.001
	95% CI Upper	0.815	−0.089	0.510	0.858	0.785	0.989
	95% CI Lower	−0.430	−0.934	−0.777	−0.306	−0.495	0.768
	Spearman's rho	0.347	−0.574	−0.092	0.294	0.313	0.921 ***
	<i>p</i> -value	0.361	0.106	0.814	0.442	0.412	<0.001
	Kendall's Tau B	0.268	−0.504	−0.081	0.171	0.275	0.840 **
	<i>p</i> -value	0.372	0.104	0.795	0.527	0.376	0.005
TLS	Pearson's r	0.367	0.357	0.756 *	−0.132	−0.286	−0.267
	<i>p</i> -value	0.331	0.345	0.018	0.735	0.456	0.487
	95% CI Upper	0.829	0.825	0.945	0.583	0.467	0.483
	95% CI Lower	−0.393	−0.402	0.184	−0.732	−0.798	−0.791
	Spearman's rho	0.371	0.357	0.756 *	−0.104	−0.286	−0.170
	<i>p</i> -value	0.325	0.345	0.018	0.791	0.456	0.662
	Kendall's Tau B	0.359	0.357	0.756 *	−0.089	−0.286	−0.164
	<i>p</i> -value	0.294	0.312	0.033	0.770	0.419	0.630

Note: \*  $p < 0.05$ —statistically significant; \*\*  $p < 0.01$ —highly statistically significant; \*\*\*  $p < 0.0001$ —strongest statistical significance.

### 3.3.2. $\alpha$ SMA\_SS Variability Is Age-Dependent but Also Influences Tumor Grade (G), TLS, and Immature Tumor Blood Vessels Dynamics for Luminal B (LB)\_BC Subtype

A direct correlation between age and  $\alpha$ SMA\_SS has been observed for the LB\_BC subtype ( $p = 0.020$ ). Our data showed that 80% of patients >50 years old had a predominant SMA\_SS of 7 and 8 compared to 50% for patients <50 years old who had a SMA\_SS of 7, but none of them had a Stromal Score of 8. Also, LB\_BC is the only BC molecular subtype where G2 is directly influenced by  $\alpha$ SMA\_SS ( $p = 0.036$ ). Two main important stromal components, TLS and immature tumor stroma blood vessels (IBV\_CD34+/SMA-), were influenced by  $\alpha$ SMA\_SS. All LB\_BC cases (100%) with a score of 5 had TLS, but only 50% of cases with a score of 6 kept the TLS presence inside tumor stroma. A percentage of 37.5% of cases scored as 7 retained TLS, but none of the cases scored as 8 presented stromal TLS. This observation was certified by an inverse correlation between  $\alpha$ SMA\_SS ( $p = 0.009$ ),  $\alpha$ SMA\_H-Score ( $p = 0.005$ ), and TLS for LB\_BC.  $\alpha$ SMA\_CAFs seem to impair or stop the development of immature stromal tumor blood vessels. We observed that the highest  $\alpha$ SMA\_SS we have corresponded to the lowest number of IBV\_CD34+/SMA-stromal vessels which were counted (an inverse significant correlation with  $p = 0.019$ ). Contrarily, the lowest CD34\_H-Score was observed, as a low number of IBV\_CD34+/SMA- was counted (direct significant correlation,  $p = 0.009$ ) (Table 2).

### 3.3.3. HER2\_BC Subtype Is CD34\_CAF-Dependent but Not Influenced by $\alpha$ SMA\_CAFs

When we assessed HER2\_BC, we observed that this subtype is exclusively related to CD34\_CAF density and CD34\_H-Score. Both parameters had lower values compared to other molecular subtypes, HER2\_BC being amongst the BC molecular subtypes with the lowest value of CD34 expression in tumor stroma cells. CD34\_CAF density and CD34\_H-Score decreased as age increases ( $p < 0.001$  for both). About 66.67% of cases had no IBV\_CD34+/SMA- stromal vessels. We found that the lack of IBV\_CD34+/SMA-stromal vessels significantly was correlated with low CD34\_CAF density ( $p < 0.001$ ) and low CD34\_H-Score ( $p < 0.001$ ). Interestingly, HER2\_BC cases with no immature stromal tumor vessels had no LVI ( $p < 0.001$ ), PrI ( $p < 0.001$ ), or recurrence ( $p < 0.001$ ) (Table 3).

### 3.3.4. Luminal B-HER2 (LB-HER2) BC Is Influenced by Both Types of CAFs, but Each of Them Had Significant Impact on Different Stromal Vascular Components and Clinic-Pathologic Parameters

Mature (MBV\_CD34+/ $\alpha$ SMA+) and immature (IBV\_CD34+/ $\alpha$ SMA-) stromal vessel density was assessed previously, and data were registered and used to study the influence of tumor stroma CAFs on their variability. As for HER2\_BC, LB-HER2 stromal IBV\_CD34+/ $\alpha$ SMA- density was highly influenced by CD34\_CAFs, but, for this subtype, all three DIA parameters (S\_CD34\_D, CD34\_SS, and CD34-H-Score) were strongly and directly correlated with IBV\_CD34+/ $\alpha$ SMA- density ( $p < 0.001$ ). Low CD34\_CAF density supported a low density of immature stromal vessels. These findings suggest that CD34\_CAFs may be tumor stromal cellular components with the potential for mesenchymal to endothelial transition followed by an angiogenic switch. Contrarily, we reported here that S\_ $\alpha$ SMA\_D was directly correlated with MBV\_CD34+/ $\alpha$ SMA+ stromal vessel density ( $p = 0.043$ ). A high survival rate was significantly correlated with high S\_ $\alpha$ SMA\_D in tumor stroma ( $p = 0.012$ ). Menopausal women had a significantly higher  $\alpha$ SMA\_H-Score compared to pre-menopausal patients ( $p = 0.013$ ) for the LB-HER2 BC subtype. A correlation matrix and correlation plot sustaining the above presented data may be seen in the overview in Table 1 and Figure 5. All detailed data related to CD34\_CAF impact on LB-HER2 BC subtype may be seen in Tables 4 and 5 and Figures 5 and 6.

**Table 2.** Correlation matrix for LB BC subtype showing significant correlations for this BC molecular subtype related to immune and vascular stromal components and SMA\_CAFs digital parameters.

		H-SCORE	S_SMA_I	S_SMA_D	S-SCORE	IMBV_CD34+/SMA-
S_SMA_I	Pearson's r	0.506 *	—			
	<i>p</i> -value	0.027	—			
	95% CI Upper	0.781	—			
	95% CI Lower	0.068	—			
	Spearman's rho	0.388	—			
	<i>p</i> -value	0.101	—			
	Kendall's Tau B	0.338	—			
	<i>p</i> -value	0.073	—			
S_SMA_D	Pearson's r	0.765 ***	0.056	—		
	<i>p</i> -value	<0.001	0.821	—		
	95% CI Upper	0.905	0.497	—		
	95% CI Lower	0.476	−0.409	—		
	Spearman's rho	0.871 ***	0.092	—		
	<i>p</i> -value	<0.001	0.707	—		
	Kendall's Tau B	0.745 ***	0.099	—		
	<i>p</i> -value	<0.001	0.654	—		
S-SCORE	Pearson's r	0.870 ***	0.685 **	0.731 ***	—	
	<i>p</i> -value	<0.001	0.001	<0.001	—	
	95% CI Upper	0.949	0.869	0.890	—	
	95% CI Lower	0.687	0.335	0.414	—	
	Spearman's rho	0.895 ***	0.603 **	0.813 ***	—	
	<i>p</i> -value	<0.001	0.006	<0.001	—	
	Kendall's Tau B	0.779 ***	0.555 **	0.722 ***	—	
	<i>p</i> -value	<0.001	0.008	<0.001	—	
IMBV_CD34+/SMA-	Pearson's r	−0.378	−0.434	−0.370	−0.532 *	—
	<i>p</i> -value	0.111	0.064	0.119	0.019	—
	95% CI Upper	0.092	0.026	0.101	−0.103	—
	95% CI Lower	−0.71	−0.742	−0.706	−0.794	—
	Spearman's rho	−0.354	−0.346	−0.352	−0.446	—
	<i>p</i> -value	0.137	0.147	0.139	0.056	—
	Kendall's Tau B	−0.187	−0.267	−0.293	−0.339	—
	<i>p</i> -value	0.285	0.179	0.149	0.079	—

Table 2. Cont.

		H-SCORE	S_SMA_I	S_SMA_D	S-SCORE	IMBV_CD34+/SMA-
TLS	Pearson's r	−0.617 **	−0.519 *	−0.396	−0.579 **	0.540 *
	<i>p</i> -value	0.005	0.023	0.094	0.009	0.017
	95% CI Upper	−0.227	−0.085	0.071	−0.170	0.798
	95% CI Lower	−0.837	−0.788	−0.720	−0.818	0.113
	Spearman's rho	−0.603 **	−0.505 *	−0.380	−0.561 *	0.544 *
	<i>p</i> -value	0.006	0.028	0.108	0.013	0.016
	Kendall's Tau B	−0.505 *	−0.482 *	−0.372	−0.519 *	0.479 *
	<i>p</i> -value	0.010	0.032	0.107	0.017	0.021
G	Pearson's r	0.280	0.367	0.331	0.484 *	−0.271
	<i>p</i> -value	0.245	0.122	0.167	0.036	0.261
	95% CI Upper	0.652	0.704	0.682	0.769	0.208
	95% CI Lower	−0.199	−0.104	−0.145	0.038	−0.646
	Spearman's rho	0.289	0.345	0.364	0.466 *	−0.421
	<i>p</i> -value	0.230	0.148	0.126	0.044	0.073
	Kendall's Tau B	0.238	0.327	0.348	0.434 *	−0.370
	<i>p</i> -value	0.221	0.140	0.125	0.043	0.070
AGE	Pearson's r	0.354	0.358	0.358	0.527 *	−0.459 *
	<i>p</i> -value	0.137	0.133	0.132	0.020	0.048
	95% CI Upper	0.696	0.699	0.699	0.792	−0.006
	95% CI Lower	−0.119	−0.115	−0.115	0.096	−0.756
	Spearman's rho	0.339	0.308	0.345	0.474 *	−0.287
	<i>p</i> -value	0.156	0.199	0.148	0.040	0.234
	Kendall's Tau B	0.226	0.238	0.287	0.360	−0.235
	<i>p</i> -value	0.190	0.222	0.151	0.057	0.194

Note. \*  $p < 0.05$ —statistically significant, \*\*  $p < 0.01$ —highly statistically significant, \*\*\*  $p < 0.001$ —strongest statistical significance.

**Table 3.** Raw data about SMA\_CAF impact on HER2 BC subtype.

		S_SMA_I	SMA_STROMAL SCORE	SMA_H-SCORE	CD34_H-SCORE	S_CD34_D	AGE	IMBV_CD34+/SMA-
SMA_STROMAL SCORE	Pearson's r	1.000 ***	—					
	<i>p</i> -value	<0.001	—					
	Spearman's rho	1.000 ***	—					
	<i>p</i> -value	<0.001	—					
	Kendall's Tau B	1.000	—					
	<i>p</i> -value	0.157	—					
SMA_H-SCORE	Pearson's r	0.814	0.814	—				
	<i>p</i> -value	0.395	0.395	—				
	Spearman's rho	0.866	0.866	—				
	<i>p</i> -value	0.333	0.333	—				
	Kendall's Tau B	0.816	0.816	—				
	<i>p</i> -value	0.221	0.221	—				
CD34_H-SCORE	Pearson's r	−0.500	−0.500	−0.910	—			
	<i>p</i> -value	0.667	0.667	0.272	—			
	Spearman's rho	−0.500	−0.500	−0.866	—			
	<i>p</i> -value	0.667	0.667	0.333	—			
	Kendall's Tau B	−0.500	−0.500	−0.816	—			
	<i>p</i> -value	0.480	0.480	0.221	—			
S_CD34_D	Pearson's r	−0.500	−0.500	−0.910	1.000 ***	—		
	<i>p</i> -value	0.667	0.667	0.272	<0.001	—		
	Spearman's rho	−0.500	−0.500	−0.866	1.000 ***	—		
	<i>p</i> -value	0.667	0.667	0.333	<0.001	—		
	Kendall's Tau B	−0.500	−0.500	−0.816	1.000	—		
	<i>p</i> -value	0.480	0.480	0.221	0.157	—		
AGE	Pearson's r	0.500	0.500	0.910	−1.000 ***	−1.000 ***	—	
	<i>p</i> -value	0.667	0.667	0.272	<0.001	<0.001	—	
	Spearman's rho	0.500	0.500	0.866	−1.000 ***	−1.000 ***	—	
	<i>p</i> -value	0.667	0.667	0.333	<0.001	<0.001	—	
	Kendall's Tau B	0.500	0.500	0.816	−1.000	−1.000	—	
	<i>p</i> -value	0.480	0.480	0.221	0.157	0.157	—	

Table 3. Cont.

		S_SMA_I	SMA_STROMAL SCORE	SMA_H-SCORE	CD34_H-SCORE	S_CD34_D	AGE	IMBV_CD34+/SMA-
MBV_CD34+/SMA+	Pearson's r	0.000	0.000	−0.581	0.866	0.866	−0.866	
	<i>p</i> -value	1.000	1.000	0.605	0.333	0.333	0.333	
	Spearman's rho	0.000	0.000	−0.500	0.866	0.866	−0.866	
	<i>p</i> -value	1.000	1.000	1.000	0.333	0.333	0.333	
	Kendall's Tau B	0.000	0.000	−0.333	0.816	0.816	−0.816	
	<i>p</i> -value	1.000	1.000	1.000	0.221	0.221	0.221	
IMBV_CD34+/SMA-	Pearson's r	−0.500	−0.500	−0.910	1.000 ***	1.000 ***	−1.000 ***	—
	<i>p</i> -value	0.667	0.667	0.272	<0.001	<0.001	<0.001	—
	Spearman's rho	−0.500	−0.500	−0.866	1.000 ***	1.000 ***	−1.000 ***	—
	<i>p</i> -value	0.667	0.667	0.333	<0.001	<0.001	<0.001	—
	Kendall's Tau B	−0.500	−0.500	−0.816	1.000	1.000	−1.000	—
	<i>p</i> -value	0.480	0.480	0.221	0.157	0.157	0.157	—
LVI	Pearson's r	−0.500	−0.500	−0.910	1.000 ***	1.000 ***	−1.000 ***	1.000 ***
	<i>p</i> -value	0.667	0.667	0.272	<0.001	<0.001	<0.001	<0.001
	Spearman's rho	−0.500	−0.500	−0.866	1.000 ***	1.000 ***	−1.000 ***	1.000 ***
	<i>p</i> -value	0.667	0.667	0.333	<0.001	<0.001	<0.001	<0.001
	Kendall's Tau B	−0.500	−0.500	−0.816	1.000	1.000	−1.000	1.000
	<i>p</i> -value	0.480	0.480	0.221	0.157	0.157	0.157	0.157
PnI	Pearson's r	−0.500	−0.500	−0.910	1.000 ***	1.000 ***	−1.000 ***	1.000 ***
	<i>p</i> -value	0.667	0.667	0.272	<0.001	<0.001	<0.001	<0.001
	Spearman's rho	−0.500	−0.500	−0.866	1.000 ***	1.000 ***	−1.000 ***	1.000 ***
	<i>p</i> -value	0.667	0.667	0.333	<0.001	<0.001	<0.001	<0.001
	Kendall's Tau B	−0.500	−0.500	−0.816	1.000	1.000	−1.000	1.000
	<i>p</i> -value	0.480	0.480	0.221	0.157	0.157	0.157	0.157
R	Pearson's r	−0.500	−0.500	−0.910	1.000 ***	1.000 ***	−1.000 ***	1.000 ***
	<i>p</i> -value	0.667	0.667	0.272	<0.001	<0.001	<0.001	<0.001
	Spearman's rho	−0.500	−0.500	−0.866	1.000 ***	1.000 ***	−1.000 ***	1.000 ***
	<i>p</i> -value	0.667	0.667	0.333	<0.001	<0.001	<0.001	<0.001
	Kendall's Tau B	−0.500	−0.500	−0.816	1.000	1.000	−1.000	1.000
	<i>p</i> -value	0.480	0.480	0.221	0.157	0.157	0.157	0.157

\*\*\*  $p < 0.001$ —strongest statistical significance.

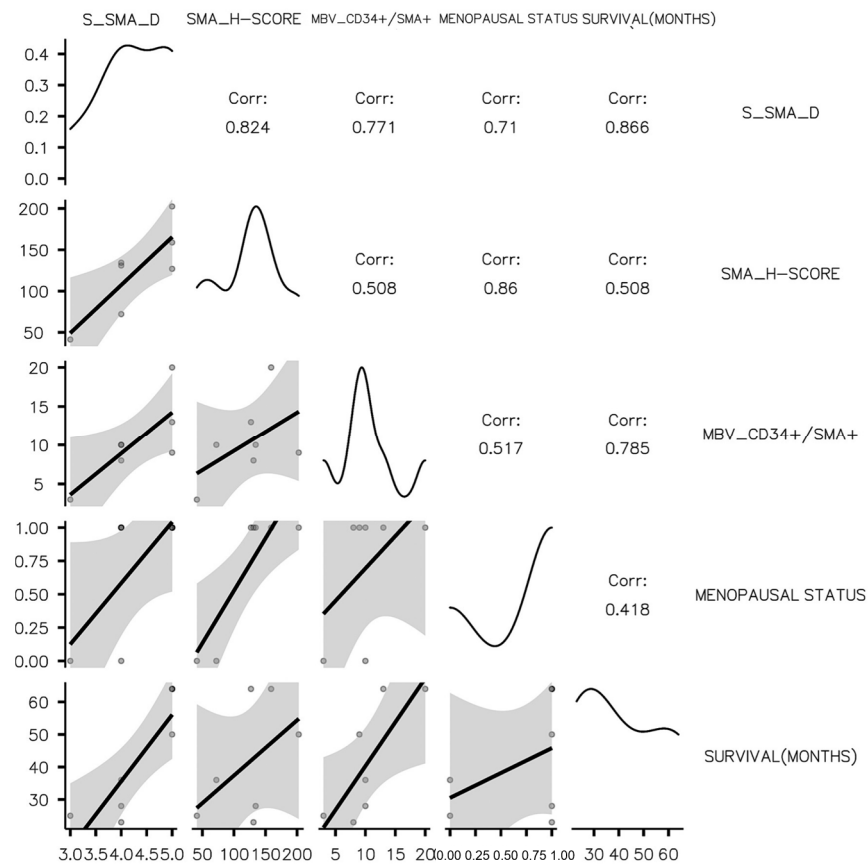


Figure 5. Plot representation of correlation matrix for the LB\_HER2 subtype related to  $\alpha$ SMA\_CAFs.

Table 4. Correlation matrix for LB\_HER2 BC showing a significant correlation between  $\alpha$ SMA\_CAFs parameters derived from DIA with tumor stroma mature blood vessels (MBV\_CD34+/SMA+), survival, and menopausal status.

		S_SMA_D	SMA_H-SCORE	MBV_CD34+/SMA+
SMA_H-SCORE	Pearson's r	0.824 *	—	—
	p-value	0.023	—	—
	95% CI Upper	0.973	—	—
	95% CI Lower	0.186	—	—
	Spearman's rho	0.694	—	—
	p-value	0.083	—	—
	Kendall's Tau B	0.620	—	—
	p-value	0.071	—	—
MBV_CD34+/SMA+	Pearson's r	0.771 *	0.508	—
	p-value	0.043	0.244	—
	95% CI Upper	0.964	0.912	—
	95% CI Lower	0.042	−0.397	—
	Spearman's rho	0.701	0.342	—
	p-value	0.080	0.452	—
	Kendall's Tau B	0.635	0.293	—
	p-value	0.068	0.362	—

Table 4. Cont.

		S_SMA_D	SMA_H-SCORE	MBV_CD34+/SMA+
MENOPAUSAL STATUS	Pearson's r	0.710	0.860 *	0.517
	p-value	0.074	0.013	0.235
	95% CI Upper	0.953	0.979	0.914
	95% CI Lower	−0.092	0.303	−0.387
	Spearman's rho	0.683	0.791 *	0.399
	p-value	0.091	0.034	0.375
	Kendall's Tau B	0.653	0.690	0.354
	p-value	0.094	0.053	0.329
SURVIVAL (MONTHS)	Pearson's r	0.866 *	0.508	0.785 *
	p-value	0.012	0.245	0.036
	95% CI Upper	0.980	0.912	0.967
	95% CI Lower	0.326	−0.397	0.079
	Spearman's rho	0.856 *	0.378	0.836 *
	p-value	0.014	0.403	0.019
	Kendall's Tau B	0.751 *	0.293	0.650 *
	p-value	0.031	0.362	0.046

S\_SMA\_D—DIA-derived density of  $\alpha$ SMA\_CAFs; SMA\_H-Score—histological score automated calculated by QuPath platform. \*  $p < 0.05$ —statistically significant.

**Table 5.** Correlation matrix for LB\_HER2 BC showing a significant correlation between CD34\_CAFs parameters derived from DIA with tumor stroma immature blood vessels (IMBV\_CD34+/SMA+), survival, and menopausal status.

		S_CD34_D	CD34_STROMAL SCORE	CD34_H-SCORE
CD34_STROMAL SCORE	Pearson's r	1.000 ***	—	—
	p-value	<0.001	—	—
	95% CI Upper	1.000	—	—
	95% CI Lower	1.000	—	—
	Spearman's rho	1.000 ***	—	—
	p-value	<0.001	—	—
	Kendall's Tau B	1.000 *	—	—
	p-value	0.014	—	—
CD34_H-SCORE	Pearson's r	0.984 ***	0.984 ***	—
	p-value	<0.001	<0.001	—
	95% CI Upper	0.998	0.998	—
	95% CI Lower	0.893	0.893	—
	Spearman's rho	0.618	0.618	—
	p-value	0.139	0.139	—
	Kendall's Tau B	0.548	0.548	—
	p-value	0.130	0.130	—
IMBV_CD34+/SMA-	Pearson's r	0.961 ***	0.961 ***	0.967 ***
	p-value	<0.001	<0.001	<0.001
	95% CI Upper	0.994	0.994	0.995
	95% CI Lower	0.753	0.753	0.785
	Spearman's rho	0.624	0.624	0.505
	p-value	0.135	0.135	0.248
	Kendall's Tau B	0.562	0.562	0.410
	p-value	0.127	0.127	0.214

\*  $p < 0.05$ —statistically significant. \*\*\*  $p < 0.001$ —strongest statistical significance.

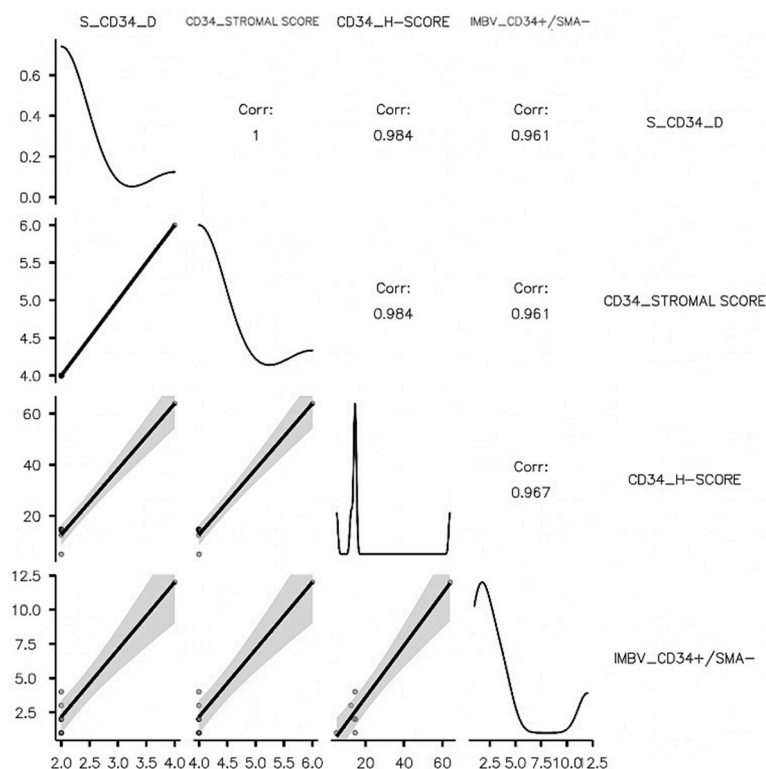


**Figure 6.** Plot representation of correlation matrix for the LB\_HER2 subtype related to CD34\_CAFs.

We consider these data to have high originality due to the lack of reports related to the LB\_HER2 BC subtype about stromal cell heterogeneity and their impact on survival and prognosis.

### 3.3.5. CD34\_CAFs Are Key Players of TNBC\_BC Stroma Influencing G, NPI, Invasion, Recurrence, and Survival

Values of the Nottingham Prognostic Index (NPI) and G seem to be CD34\_CAF-dependent on TNBC\_BC. An NPI value of 7 corresponded to a CD34\_SS of 4 while an NPI value of 8 significantly overlapped with a CD34\_SS of 5 and thus gave us a global significant correlation between NPI and CD34\_SS for a value of  $p = 0.009$ . All G2 cases had a CD34\_SS of 4 while 71.42% of G3 cases had a CD34\_SS of 5. To these correspondences, a significant correlation has been reported ( $p = 0.024$ ). For survival and menopausal status, a partial, low-significance correlation has been registered related to CD34\_SS and CD34\_H-Score. PnI and recurrence were highly dependent on the presence of CD34\_CAFs for a correlation with all three parameters ( $p = 0.009$  for S\_CD34\_D;  $p = 0.032$  for CD34\_SS; and  $p = 0.002$  for CD34\_H-Score), while LVI had a significant correlation with CD34\_SS only. We did not detect any significant impact of CD34\_CAFs on the tumor stromal vascular compartment for the TNBC BC subtype based on DIA parameters.

## 4. Discussion

The impact of the tumor–stroma ratio on prognosis and therapy response is a relatively new topic in BC research field [32,33,43] in recent years. Its diagnostic and prognostic value increased by association of tumor stroma ratio with other clinic-pathologic parameters such as multiparametric MRI findings [43], oncogenic proteins [44], axillary lymph node metastasis [45], or TNM staging [46]. The tumor–stroma ratio was evaluated using different DIA software, but it seems that one of the favorites is the QuPath analysis platform due to its facilities covering a wide spectrum of needs for researchers who assess microscopic images with an emphasis on tumor stroma [38,39,47]. We also chose the QuPath platform due to its tools' ability to sharply detect and label stromal fibroblasts and automatically perform stromal scoring and H-Score. By its versatile functions for choosing cell parameters

but also three thresholds for staining intensity, the QuPath platform provided us with a unique tool for detection and quantification of stromal CAFs based on both morphological and immunohistochemical parameters. These proved to be very useful for our following analysis of CAF impact on clinic-pathologic parameters due to several correlations found in the present study.

Divergent expression of CD34 and  $\alpha$ SMA in normal breast stromal fibroblasts and tumor stroma CAFs was previously observed and reported by several authors [6,19,48,49]. CD34 positive fibroblasts' presence was highly associated with normal breast stroma, while  $\alpha$ SMA-positive CAFs were intensely discussed as being specific to the BC tumor stroma [6,19,48,49]. For BC where CD34-positive stromal cells are present inside the tumor stroma, some authors suggested that CD34-positive BC stromal cells/telocytes are precursors for  $\alpha$ SMA-positive stromal CAFs [27], and this may explain divergent expression of two markers from the ability of CD34-positive stromal cells to dedifferentiate into  $\alpha$ SMA-positive CAFs. Also, CD34-positive stromal cells have been reported to be a source of mesenchymal cells [25], which may have the ability to differentiate into several cell types from endothelial cells [24] to myofibroblasts in BC stroma [50].

Because of CD34-positive CAFs' low density in the BC stromal compartment, their conventional microscopic objective assessment is practically impossible. Several BC studies reported the lack of CD34-positive CAFs by using conventional microscopy instead of using automated quantification. On the other hand, the CD34 antigen is also expressed in the endothelium of tumor stromal blood vessels and is highly associated with tumor angiogenesis instead of its CAF expression [51–53]. The above evidence supports the prognostic role of CD34-positive CAFs as versatile cells with a high ability for dedifferentiation in various heterogeneous cells from stromal to malignant ones. This uncontrolled and less elucidated dedifferentiation may be a trigger for therapy resistance development or for the development of malignant cells with a high ability for invasion and metastasis. An accurate and correct assessment of CD34\_CAFs is not possible without digital image analysis. Thus, we consider their assessment by using IHC and DIA to be necessary as a routine procedure during initial microscopic evaluation of any BC case to predict a potential bad prognosis or development of resistance to therapy. Our recommendation is supported by our findings and by some of the literature data pointing out CD34\_CAFs' role in BC. Recently, Westhoff and collaborators reported the prognostic relevance of CD34\_CAF loss in BC [17]. Their semiquantitative conventional grading results referred to invasive lobular carcinoma (ILC) as being related to its morphological subtypes, the presence of metastasis, and pTNM staging parameters without any mention of BC molecular subtypes. The present study partially confirmed their results but is closely related to BC molecular subtypes. We found that a low CD34\_CAF density was significantly correlated with a low survival rate for the LA subtype. Other authors previously mentioned that CD34\_CAFs' presence may exert a positive role in various tumor types such as lung cancer [54], pancreatic neoplastic lesions [55], or cervical cancer [56], most likely due to their involvement in tumor stroma remodeling with no relation to prognostic or clinical parameters. Thus, a CD34\_CAF variability assessment may stratify BC patients with the LA subtype into different survival rate subgroups with a possible different response to therapy and disease-free survival.

There are several data points about  $\alpha$ SMA\_CAFs' involvement in the development of resistance to Trastuzumab [57–59], but there are none about CD34\_CAFs' influence on the HER2 subtype of BC. By applying DIA analysis of IHC-stained slides, we found that the lowest CD34\_CAFs\_D was registered inside the stroma of the HER2-positive subtype. This seems to influence the development of a low number of tumor stroma blood vessels of an immature type which in turn may limit LVI and PnI according to our findings. No data about a significant correlation between CD34\_CAFs\_D, tumor stroma vessels, and invasion is available at this time in the literature for BC, and thus, our findings will need further studies for a complete characterization of CD34\_CAFs' impact on therapy and prognosis for the HER2 subtype. Indirect evidence which may support our correlation between low CD34\_CAFs\_D and low immature tumor stroma blood vessel (IBV\_CD34+/ $\alpha$ SMA-)

density was published by San Martin et al. in 2014. They hypothesized that CD34\_CAFs' recruitment by the tumor stroma is achieved from the stromal microvasculature [60]. As low as microvascular density is, low CD34\_CAFs\_D is observed as we also reported here. Interestingly, this interrelation between IBV\_CD34+/αSMA- and CD34\_CAFs was also found for the LB and LB-HER2 subtypes but not for TNBC. The strongest significant correlation between all CD34\_CAFs parameters and IBV\_CD34+/αSMA- was observed for the LB-HER2 subtype in the present study. All DIA-assessed CD34\_CAFs parameters showed a strong correlation with stromal immature blood vessels. Based on our analysis, we may partially confirm the reactive vascular hypothesis of San Martin et al. [60], with the novelty of the present study being that this confirmation characterized HER2 and LB-HER2 BC subtypes only.

But the highest significance of CD34\_CAF DIA assessment was noticed for TNBC\_BC in the present study not only with impact on other stromal components but also related to tumor grade and NPI. Recently, Wu et al. [61] described the TNBC stroma heterogeneity related to the presence of four types of CAFs and reported their influence on tumor immune evasion ability but not on invasion or other prognostic markers. They defined CD34\_CAFs as inflammatory CAFs (iCAF) and proved that they are distributed far from malignant areas intermixed with a heterogeneous population of inflammatory cells [56]. In the same paper, the authors mentioned the iCAF related to the enrichment of growth factor gene ontologies with a strong upregulation of crosstalk via the FGF, BMP, HGF, and IGF1 pathways through the corresponding receptors distributed in malignant cells and endothelial cells. This crosstalk is known to induce BC cell proliferation and invasion [56] in TNBC\_BC. Their findings support our significant correlations found between CD34\_CAF DIA parameters (density, stromal score, and H-Score) and G, NPI, LVI, and PnI specific to TNBC\_BC. To the best of our knowledge, we were not able to find any literature data which may support CD34\_CAFs' association with microscopic and/or clinico-pathologic parameters in the TNBC\_BC subgroup, specifically most likely due to the lack of CD34\_CAFs in a digital image analysis program. This is one more reason sustaining DIA CD34\_CAFs' utility for the evaluation improvement of TNBC\_BC patients. The same study by Wu et al. stated that the classical angiogenic pathways were enriched for iCAF, and thus, iCAF induce tumor neovascularization. This also may support our findings related to the interrelation between CD34\_CAFs (iCAF) and IBV\_CD34+/SMA- for some BC molecular subtypes [61].

Myofibroblast-like CAFs (myCAF) are another type of CAF described in the BC stromal compartment, but, compared with iCAF, myCAF are located at the tumor–stroma interface and invasion front, close to the tumor area [56]. For IHC, the most common marker used to identify myCAF is the αSMA antibody which we also used in the present study. myCAF marker αSMA accumulation in the tumor stromal fibroblast has a poor prognostic significance for BC patients [62,63]. αSMA\_CAFs are responsible not only for poor prognosis in primary malignancy, but also, they are also recently described as being responsible for poor prognosis and a high recurrence rate of brain metastases [64]. These effects were associated especially with αSMA and PDGFR-β expression in stromal myofibroblast-like cells. αSMA\_CAFs induce tumor stroma remodeling by targeting several stromal components from stromal vessels to collagen synthesis, inflammatory cells, and tertiary lymphoid structures (TLSs). αSMA\_CAFs modulate the immune tumor microenvironment of several cancer types [65], but the interplay in between αSMA\_CAFs and TLSs is less elucidated in malignancies, including breast cancer also.

The prevalence of stromal myofibroblasts (i.e., αSMA-positive fibroblasts) in human breast cancers is related to aggressive adenocarcinomas and predicts human disease recurrence [66,67]. Costa et al. identified four types of CAFs in human breast cancer stroma (CAF-S1 to CAF-S4) [68], but only two of them are described to be highly positive for αSMA (CAF-S1 and CAF-S4). CAF-S3 was characterized to having negative to low expression of αSMA\_CAFs [68]. Thus, differences in between αSMA immune expression must be quantified by using the digital image analysis. This may be a simple method applied to differentiate between various αSMA\_CAF types in routine IHC combined with DIA at the

first evaluation of BC specimens. Differential assessment of  $\alpha$ SMA expression intensity for CAFs (performed by DIA to obtain stromal score like has been described in the present study) may suggest CAFs' heterogeneity from BC stroma and may recommend additional tests to predict poor prognosis and/or recurrence by pathologists.

It has been proved that different CAF types are heterogeneously distributed in between BC molecular subtypes [63]. This is in line with our findings. We reported here not only differences between CD34\_CAFs and  $\alpha$ SMA\_CAFs' impact in BC but also the interrelation with other stromal components as tumor stroma vasculature and immune cells or clinic-pathologic parameters. One new finding arising from the present study was the significant association of age with  $\alpha$ SMA\_SS and/or  $\alpha$ SMA\_H-Score for LA\_BC and LB\_BC subtypes. These findings suggest that age-related differences may influence the BC patient's stroma reaction to malignant conditions based on CD34\_CAFs and  $\alpha$ SMA\_CAFs.

The impact of CAFs on vasculature and the tumor stroma immune microenvironment is less studied. By using double immunostaining for endothelial (CD34) and perivascular ( $\alpha$ SMA) markers, we were able to assess not only stromal vessels' maturation grade and types but also their interrelation with  $\alpha$ SMA\_CAFs. In the same paper by Costa et al., the authors pointed out the differences between CAF-S1 and CAF-S4 at the transcriptomic level, suggesting a different role of these two types of  $\alpha$ SMA-expressing CAFs [68]. This may explain in part our contradictory results found for  $\alpha$ SMA\_CAFs' interrelations with TLSs between LA\_BC and LB\_BC subtypes. For LA\_BC, our results suggest that  $\alpha$ SMA\_CAFs stimulate TLS formation by a significant direct correlation between these two parameters. These CAFs present in LA-BC are most probably the CAF-S1 type known for its ability to attract and instruct immune cells through a phenotype such as that of cells composing TLSs, and by this mechanism they stimulate TLS organization. Until the present study, this was proved for TNBC\_BC but not for LA\_BC. Based on our findings, further studies will be needed to elucidate if TLSs' presence in LA\_BC may split this molecular subtype into two subgroups with a possible different response to antitumor immune therapy. The interrelation between CAFs and TLSs has been also reported for lung cancer [69]. Bonneau et al. [70] created a CAF types of distribution map for luminal A and B early breast cancer, linking their accumulation to recurrence. They reported that CAF-S1 enrichment of early luminal BC is a risk factor for recurrence, being independent of age and epithelial, immune, and vascular features. Our data are partially in contradiction with previous findings. We found that  $\alpha$ SMA\_CAFs in LA\_BC are highly and significantly related to the TLS presence (an immune component of tumor stroma) and influenced by age, but we did not find any impact on recurrence and invasion for LA\_BC. The interrelation between age and  $\alpha$ SMA\_CAF Stromal Score was kept for LB\_BC also. But the most original findings of the present paper may be considered that  $\alpha$ SMA\_CAFs seem to negatively influence tumor stroma immature vessels and TLS development in LB\_BC. We found that TLSs' presence drastically decreased with increased  $\alpha$ SMA\_SS, suggesting an inverse correlation between them for LB\_BC compared to LA\_BC where we found a direct significant correlation. The discrepancies between the two types of luminal BC may be explained in part by the presence of different CAF phenotypes. CAF-S1 and CAF-S4 are two types of fibroblasts which are both positive for  $\alpha$ SMA, but several differences related to traits other than their markers have been reported [68]. CAF-S1 has upregulated genes involved in cell adhesion, extracellular matrix organization, and immune response while CAF-S4 is responsible for muscle contraction, regulation of the actin cytoskeleton, and oxidative metabolism [68].

Based on the above evidence related to distinct CAF functions, we may speculate that CAF-S1's associated function as a promoter of TLS immune cells' development may sustain our findings related to a direct correlation between TLSs and  $\alpha$ SMA-CAF found for LA\_BC. Contrarily, an inverse correlation found between the same factors for LB\_BC may suggest the presence of another CAF subset positive for  $\alpha$ SMA, CAF-S4. This subset has no immunogenic role, but it is called a perivascular type according to its phenotype and function [68,71]. The non-immunogenic role of CAF-S4 sustains the inverse correlation found in the present study between TLSs and  $\alpha$ SMA-CAF. Their perivascular phenotype

may suggest their contribution to a rapid maturation of tumor stroma blood vessels during tumor angiogenesis. This is in accordance with our findings for LB\_BC where the inverse correlation between IBV\_CD34+/SMA- stromal vessels and  $\alpha$ SMA-SS has been reported. Another hypothesis related to these two inverse correlations found for LB\_BC may be the mechanical impact of CAF-S4 on tumor stroma components related to their certified contractility ability. Changes in the tumor stroma stiffness related to CAF-S4 contractility may impair stromal immune cell trafficking and vascular network expansion.

The interrelation between TLSs and tumor stroma blood vessels was recently reported by our team [72] and together with the findings from the present study may sustain the expansion of BC stroma research by integrating as many stromal components as we have for a better understanding of tumor stroma heterogeneity.

A limited number of papers assessed both  $\alpha$ SMA\_CAF and CD34\_CAF interplay in breast cancer stroma [73], with most of them being related to the diagnosis of breast pathologic conditions [74–76] other than invasive breast cancer molecular subtypes. This may be the main reason why CD34\_CAFs' role in highly aggressive BC subtypes such as HER2 and TNBC is underestimated in its relationship with other clinic-pathologic parameters and stromal vascular and immune components.

The identification of novel CAF biomarkers is a continuously growing research field for different cancers [77–79]. Similar to CD34\_CAFs which have the ability to transdifferentiate into endothelial cells which may favor new blood vessel development, podoplanin-positive CAFs [80], which recently received more attention in breast cancer, may be assessed as potential precursors for the development of new tumor lymphatics, for promoting tumor progression invasion and metastasis, or for serving as a target for personalized therapy [81].

Due to the small geographic area where BC cases were collected and due to the lack of a national database for research, the number of cases selected for the present study might seem small. This could be considered as a limitation of the present study, but it may be partially counterbalanced by the new original findings with special emphasis on CD34\_CAFs' different impact on BC molecular subtypes and both CD34\_CAFs' and SMA\_CAFs' interrelation with other stromal components. The validation of our results by further studies on a large cohort of cases could be developed starting from our data.

## 5. Conclusions

The present paper demonstrated that both  $\alpha$ SMA\_CAFs and CD34\_CAFs have a significant impact on tumor invasion, metastasis, recurrence, and survival differently in between BC molecular subtypes through their interplay with other stromal components (as immune cells and vascular network), being influenced by age, menopausal status, tumor grade, and NPI. Our results together with previously published data strongly suggest a stringent need for BC specimens' initial evaluation improvement by using IHC techniques combined with DIA methods applied not only to tumor epithelial components assessment but also to cellular heterogeneity of BC stromal fibroblasts. In this light, CD34\_CAF assessment should receive similar attention as  $\alpha$ SMA\_CAFs have already received. Our data revealed that, despite their low density in tumor stroma, CD34\_CAFs have a significant influence on LVI, PnI, NPI, G, recurrence, and survival in some of the most aggressive BC subtypes such as HER2 and TNBC. Scattered and elusive data found in the literature related to CD34\_CAFs' impact may be due to the lack of using DIA for their assessment. We proved here that CD34-CAFs should be mandatory for assessment together with  $\alpha$ SMA\_CAFs by using special DIA software because they may influence important clinic-pathologic parameters dependent on BC molecular subtypes. The data about the potential impact of CD34\_CAFs on BC clinic-pathologic parameters highlighted on the present paper, together with our findings about CD34\_CAFs' and  $\alpha$ SMA\_CAFs' impact on the LB-HER2 BC molecular subtype may be considered the most original parts of the present study.

**Author Contributions:** Conceptualization, A.C.B. and M.P.F.; methodology, A.C.B., M.P., M.-M.M. and M.P.F.; software, M.-M.M.; validation, A.M.C., E.C., E.M. and M.P.F.; formal analysis, L.T. and M.-M.M.; investigation, A.C.B. and M.P.F.; resources, L.T.; data curation, A.M.C. and M.P.F.; writing—original draft preparation, A.C.B.; writing—review and editing, A.M.C.; supervision, A.M.C., E.C. and E.M.; project administration, M.-M.M. All authors have read and agreed to the published version of the manuscript.

**Funding:** This research was funded by “Victor Babeş University of Medicine Research Department, Timisoara, Romania”.

**Institutional Review Board Statement:** The study was conducted in accordance with the Declaration of Helsinki and approved by the Ethics Committee of “Victor Babeş University of Medicine Research Department, Timisoara, Romania” (No. 49/28.09.2018) for studies involving humans.

**Informed Consent Statement:** Informed consent was obtained from all subjects involved in the study.

**Data Availability Statement:** The data can be shared up on request.

**Acknowledgments:** We are grateful to Victor Babeş University of Medicine and Pharmacy Timisoara Romania administrative staff for excellent logistic and infrastructure supporting our research work. Special gratitude to Emanuel Ciprian Onica and Raluca Amalia Ceausu for their excellent skills during slide processing by histological and immunohistochemical techniques.

**Conflicts of Interest:** The authors have no conflict of interest.

## References

- Zheng, S.; Zou, Y.; Tang, Y.; Yang, A.; Liang, J.Y.; Wu, L.; Tian, W.; Xiao, W.; Xie, X.; Yang, L.; et al. Landscape of cancer-associated fibroblasts identifies the secreted biglycan as a protumor and immunosuppressive factor in triple-negative breast cancer. *Oncoimmunology* **2022**, *11*, 2020984. [[CrossRef](#)] [[PubMed](#)]
- Xie, J.; Zheng, S.; Zou, Y.; Tang, Y.; Tian, W.; Wong, C.W.; Wu, S.; Ou, X.; Zhao, W.; Cai, M.; et al. Turning up a new pattern: Identification of cancer-associated fibroblast-related clusters in TNBC. *Front. Immunol.* **2022**, *13*, 1022147. [[CrossRef](#)] [[PubMed](#)]
- Zheng, S.; Liang, J.Y.; Tang, Y.; Xie, J.; Zou, Y.; Yang, A.; Shao, N.; Kuang, X.; Ji, F.; Liu, X.; et al. Dissecting the role of cancer-associated fibroblast-derived biglycan as a potential therapeutic target in immunotherapy resistance: A tumor bulk and single-cell transcriptomic study. *Clin. Transl. Med.* **2023**, *13*, e1189. [[CrossRef](#)] [[PubMed](#)]
- Zou, Y.; Ye, F.; Kong, Y.; Hu, X.; Deng, X.; Xie, J.; Song, C.; Ou, X.; Wu, S.; Wu, L.; et al. The Single-Cell Landscape of Intratumoral Heterogeneity and The Immunosuppressive Microenvironment in Liver and Brain Metastases of Breast Cancer. *Adv. Sci.* **2023**, *10*, e2203699. [[CrossRef](#)]
- Zhang, D.; Zhang, Y.; Zou, X.; Li, M.; Zhang, H.; Du, Y.; Wang, J.; Peng, C.; Dong, C.; Hou, Z. CHST2-mediated sulfation of MECA79 antigens is critical for breast cancer cell migration and metastasis. *Cell Death Dis.* **2023**, *14*, 288. [[CrossRef](#)]
- Cimpean, A.M.; Raica, M.; Narița, D. Diagnostic significance of the immunoexpression of CD34 and smooth muscle cell actin in benign and malignant tumors of the breast. *Rom. J. Morphol. Embryol.* **2005**, *46*, 123–129.
- Barth, P.J.; Ebrahimsade, S.; Ramaswamy, A.; Moll, R. CD34<sup>+</sup> fibrocytes in invasive ductal carcinoma, ductal carcinoma in situ, and benign breast lesions. *Virchows Arch.* **2002**, *440*, 298–303. [[CrossRef](#)]
- Yazhou, C.; Wenlv, S.; Weidong, Z.; Licun, W. Clinicopathological significance of stromal myofibroblasts in invasive ductal carcinoma of the breast. *Tumor Biol.* **2004**, *25*, 290–295. [[CrossRef](#)]
- Chauhan, H.; Abraham, A.; Phillips, J.R.; Pringle, J.H.; Walker, R.A.; Jones, J.L. There is more than one kind of myofibroblast: Analysis of CD34 expression in benign, in situ, and invasive breast lesions. *J. Clin. Pathol.* **2003**, *56*, 271–276. [[CrossRef](#)]
- Catteau, X.; Simon, P.; Vanhaeverbeek, M.; Noël, J.C. Variable stromal periductular expression of CD34 and smooth muscle actin (SMA) in intraductal carcinoma of the breast. *PLoS ONE* **2013**, *8*, e57773. [[CrossRef](#)]
- Catteau, X.; Simon, P.; Jondet, M.; Vanhaeverbeek, M.; Noël, J.C. Quantification of stromal reaction in breast carcinoma and its correlation with tumor grade and free progression survival. *PLoS ONE* **2019**, *14*, e0210263. [[CrossRef](#)]
- Artacho-Cordón, A.; Artacho-Cordón, F.; Ríos-Arrabal, S.; Calvente, I.; Núñez, M.I. Tumor microenvironment and breast cancer progression: A complex scenario. *Cancer Biol. Ther.* **2012**, *13*, 14–24. [[CrossRef](#)]
- Martins, D.; Schmitt, F. Microenvironment in breast tumorigenesis: Friend or foe? *Histol. Histopathol.* **2019**, *34*, 13–24. [[CrossRef](#)]
- Onuchic, V.; Hartmaier, R.J.; Boone, D.N.; Samuels, M.L.; Patel, R.Y.; White, W.M.; Garovic, V.D.; Oesterreich, S.; Roth, M.E.; Lee, A.V.; et al. Epigenomic Deconvolution of Breast Tumors Reveals Metabolic Coupling between Constituent Cell Types. *Cell Rep.* **2016**, *17*, 2075–2086. [[CrossRef](#)]
- Jung, Y.Y.; Lee, Y.K.; Koo, J.S. Expression of cancer-associated fibroblast-related proteins in adipose stroma of breast cancer. *Tumor Biol.* **2015**, *36*, 8685–8695. [[CrossRef](#)]
- Andrade de Oliveira, K.; Sengupta, S.; Yadav, A.K.; Clarke, R. The complex nature of heterogeneity and its roles in breast cancer biology and therapeutic responsiveness. *Front. Endocrinol.* **2023**, *14*, 1083048. [[CrossRef](#)]

17. Westhoff, C.C.; Jank, P.; Jacke, C.O.; Albert, U.S.; Ebrahimsade, S.; Barth, P.J.; Moll, R. Prognostic relevance of the loss of stromal CD34 positive fibroblasts in invasive lobular carcinoma of the breast. *Virchows Arch.* **2020**, *477*, 717–724. [[CrossRef](#)]
18. Westhoff, C.C.; Jacke, C.O.; Albert, U.S.; Moll, R. Stromal subtypes of invasive lobular carcinoma of the breast: Absence of CD34-positive stromal fibrocytes correlate with presence of  $\alpha$ -smooth muscle actin-positive myofibroblasts. In *Der Pathologe*; Moch, H., Ed.; Springer: Berlin/Heidelberg, Germany, 2018; Volume 39, (Suppl. S2).
19. Dzobo, K.; Senthebane, D.A.; Dandara, C. The Tumor Microenvironment in Tumorigenesis and Therapy Resistance Revisited. *Cancers* **2023**, *15*, 376. [[CrossRef](#)]
20. Forsare, C.; Vistrand, S.; Ehinger, A.; Lövgren, K.; Rydén, L.; Fernö, M.; Narbe, U. The Prognostic Role of Intratumoral Stromal Content in Lobular Breast Cancer. *Cancers* **2022**, *14*, 941. [[CrossRef](#)]
21. Elwakeel, E.; Weigert, A. Breast Cancer CAFs: Spectrum of Phenotypes and Promising Targeting Avenues. *Int. J. Mol. Sci.* **2021**, *22*, 11636. [[CrossRef](#)]
22. Díaz-Flores, L.; Gutiérrez, R.; García, M.P.; González, M.; Sáez, F.J.; Aparicio, F.; Díaz-Flores, L., Jr.; Madrid, J.F. Human resident CD34<sup>+</sup> stromal cells/telocytes have progenitor capacity and are a source of  $\alpha$ SMA<sup>+</sup> cells during repair. *Histol. Histopathol.* **2015**, *30*, 615–627. [[CrossRef](#)] [[PubMed](#)]
23. Hanley, C.J.; Waise, S.; Ellis, M.J.; Lopez, M.A.; Pun, W.Y.; Taylor, J.; Parker, R.; Kimbley, L.M.; Chee, S.J.; Shaw, E.C.; et al. Single-cell analysis reveals prognostic fibroblast subpopulations linked to molecular and immunological subtypes of lung cancer. *Nat. Commun.* **2023**, *14*, 387. [[CrossRef](#)] [[PubMed](#)]
24. Díaz-Flores, L.; Gutiérrez, R.; González-Gómez, M.; García, M.D.P.; Palmas, M.; Carrasco, J.L.; Madrid, J.F.; Díaz-Flores, L., Jr. Delimiting CD34<sup>+</sup> Stromal Cells/Telocytes Are Resident Mesenchymal Cells That Participate in Neovessel Formation in Skin Kaposi Sarcoma. *Int. J. Mol. Sci.* **2023**, *24*, 3793. [[CrossRef](#)] [[PubMed](#)]
25. Díaz-Flores, L.; Gutiérrez, R.; García, M.P.; Sáez, F.J.; Díaz-Flores, L., Jr.; Valladares, F.; Madrid, J.F. CD34<sup>+</sup> stromal cells/fibroblasts/fibrocytes/telocytes as a tissue reserve and a principal source of mesenchymal cells. Location, morphology, function and role in pathology. *Histol. Histopathol.* **2014**, *29*, 831–870. [[CrossRef](#)] [[PubMed](#)]
26. Díaz-Flores, L.; Gutiérrez, R.; García, M.P.; González-Gómez, M.; Rodríguez-Rodríguez, R.; Hernández-León, N.; Díaz-Flores, L., Jr.; Carrasco, J.L. Cd34<sup>+</sup> Stromal Cells/Telocytes in Normal and Pathological Skin. *Int. J. Mol. Sci.* **2021**, *22*, 7342. [[CrossRef](#)]
27. Díaz-Flores, L.; Gutiérrez, R.; González-Gómez, M.; García, M.P.; Díaz-Flores, L., Jr.; Carrasco, J.L.; Martín-Vasallo, P. CD34<sup>+</sup> Stromal Cells/Telocytes as a Source of Cancer-Associated Fibroblasts (CAFs) in Invasive Lobular Carcinoma of the Breast. *Int. J. Mol. Sci.* **2021**, *22*, 3686. [[CrossRef](#)]
28. Bonacho, T.; Rodrigues, F.; Liberal, J. Immunohistochemistry for diagnosis and prognosis of breast cancer: A review. *Biotech. Histochem.* **2020**, *95*, 71–91. [[CrossRef](#)]
29. Ray, U.; Pathoulas, C.L.; Thirusangu, P.; Purcell, J.W.; Kannan, N.; Shridhar, V. Exploiting LRRC15 as a Novel Therapeutic Target in Cancer. *Cancer Res.* **2022**, *82*, 1675–1681. [[CrossRef](#)]
30. Chen, X.; Song, E. Turning foes to friends: Targeting cancer-associated fibroblasts. *Nat. Rev. Drug Discov.* **2019**, *18*, 99–115. [[CrossRef](#)]
31. Jiang, P.; Chen, Y.; Liu, B. Prognostic Efficacy of Tumor-Stroma Ratio in Women with Breast Cancer: A Meta-Analysis of Cohort Studies. *Front. Oncol.* **2021**, *11*, 731409. [[CrossRef](#)]
32. Yan, D.; Ju, X.; Luo, B.; Guan, F.; He, H.; Yan, H.; Yuan, J. Tumour stroma ratio is a potential predictor for 5-year disease-free survival in breast cancer. *BMC Cancer* **2022**, *22*, 1082. [[CrossRef](#)]
33. Le, M.K.; Odate, T.; Kawai, M.; Oishi, N.; Kondo, T. Investigating the role of core needle biopsy in evaluating tumor-stroma ratio (TSR) of invasive breast cancer: A retrospective study. *Breast Cancer Res. Treat.* **2023**, *197*, 113–121. [[CrossRef](#)]
34. Xu, Q.; Chen, Y.Y.; Luo, Y.H.; Zheng, J.S.; Lin, Z.H.; Xiong, B.; Wang, L.W. Proposal of an automated tumor-stromal ratio assessment algorithm and a nomogram for prognosis in early-stage invasive breast cancer. *Cancer Med.* **2023**, *12*, 131–145. [[CrossRef](#)]
35. Qian, X.; Xiao, F.; Chen, Y.Y.; Yuan, J.P.; Liu, X.H.; Wang, L.W.; Xiong, B. Computerized Assessment of the Tumor-stromal Ratio and Proposal of a Novel Nomogram for Predicting Survival in Invasive Breast Cancer. *J. Cancer* **2021**, *12*, 3427–3438. [[CrossRef](#)]
36. Hanna, M.G.; Pantanowitz, L.; Evans, A.J. Overview of contemporary guidelines in digital pathology: What is available in 2015 and what still needs to be addressed? *J. Clin. Pathol.* **2015**, *68*, 499–505. [[CrossRef](#)]
37. Samuelson, M.I.; Chen, S.J.; Boukhar, S.A.; Schnieders, E.M.; Walhof, M.L.; Bellizzi, A.M.; Robinson, R.A.; Rajan, K.D.A. Rapid Validation of Whole-Slide Imaging for Primary Histopathology Diagnosis. *Am. J. Clin. Pathol.* **2021**, *155*, 638–648. [[CrossRef](#)]
38. Millar, E.K.; Browne, L.H.; Beretov, J.; Lee, K.; Lynch, J.; Swarbrick, A.; Graham, P.H. Tumour Stroma Ratio Assessment Using Digital Image Analysis Predicts Survival in Triple Negative and Luminal Breast Cancer. *Cancers* **2020**, *12*, 3749. [[CrossRef](#)]
39. Wu, D.; Hacking, S.M.; Chavarria, H.; Abdelwahed, M.; Nasim, M. Computational portraits of the tumoral microenvironment in human breast cancer. *Virchows Arch.* **2022**, *481*, 367–385. [[CrossRef](#)]
40. Lumongga, F.; Dharmajaya, R.; Siregar, K.B.; Delyuzar; Handjari, D.R.; Jusuf, N.K.; Munir, D.; Asrul. Correlation between Intensity of Vimentin Immuno-expression in Young Women with Triple Negative Breast Cancer and Its Clinicopathological Parameters. *Med. Arch.* **2022**, *76*, 454–457. [[CrossRef](#)]
41. Bankhead, P.; Loughrey, M.B.; Fernández, J.A.; Dombrowski, Y.; McArt, D.G.; Dunne, P.D.; McQuaid, S.; Gray, R.T.; Murray, L.J.; Coleman, H.G.; et al. QuPath: Open source software for digital pathology image analysis. *Sci. Rep.* **2017**, *7*, 16878. [[CrossRef](#)]

42. Available online: <https://pubmed.ncbi.nlm.nih.gov/?term=QuPath+breast+stroma> (accessed on 22 March 2023).
43. Yamaguchi, K.; Hara, Y.; Kitano, I.; Hamamoto, T.; Kiyomatsu, K.; Yamasaki, F.; Egashira, R.; Nakazono, T.; Irie, H. Tumor-stromal ratio (TSR) of invasive breast cancer: Correlation with multi-parametric breast MRI findings. *Br. J. Radiol.* **2019**, *92*, 20181032. [[CrossRef](#)] [[PubMed](#)]
44. Lee, Y.; Bae, S.J.; Eun, N.; Ahn, S.G.; Jeong, J.; Cha, Y.J. Correlation of Yes-Associated Protein 1 with Stroma Type and Tumor Stiffness in Hormone-Receptor Positive Breast Cancer. *Cancers* **2022**, *14*, 4971. [[CrossRef](#)]
45. Vangangelt, K.M.H.; Tollenaar, L.S.A.; van Pelt, G.W.; de Kruijff, E.M.; Dekker, T.J.A.; Kuppen, P.J.K.; Tollenaar, R.A.E.M.; Mesker, W.E. The prognostic value of tumor-stroma ratio in tumor-positive axillary lymph nodes of breast cancer patients. *Int. J. Cancer* **2018**, *143*, 3194–3200. [[CrossRef](#)] [[PubMed](#)]
46. Xu, Q.; Yuan, J.P.; Chen, Y.Y.; Zhang, H.Y.; Wang, L.W.; Xiong, B. Prognostic Significance of the Tumor-Stromal Ratio in Invasive Breast Cancer and a Proposal of a New Ts-TNM Staging System. *J. Oncol.* **2020**, *2020*, 9050631. [[CrossRef](#)] [[PubMed](#)]
47. Zheng, Q.; Jiang, Z.; Ni, X.; Yang, S.; Jiao, P.; Wu, J.; Xiong, L.; Yuan, J.; Wang, J.; Jian, J.; et al. Machine Learning Quantified Tumor-Stroma Ratio Is an Independent Prognosticator in Muscle-Invasive Bladder Cancer. *Int. J. Mol. Sci.* **2023**, *24*, 2746. [[CrossRef](#)]
48. Frisbie, L.; Buckanovich, R.J.; Coffman, L. Carcinoma-Associated Mesenchymal Stem/Stromal Cells: Architects of the Pro-tumorigenic Tumor Microenvironment. *Stem Cells* **2022**, *40*, 705–715. [[CrossRef](#)]
49. Xu, M.; Zhang, T.; Xia, R.; Wei, Y.; Wei, X. Targeting the tumor stroma for cancer therapy. *Mol. Cancer* **2022**, *21*, 208. [[CrossRef](#)]
50. Mishra, P.J.; Banerjee, D. Visualizing Activated Myofibroblasts Resulting from Differentiation of Mesenchymal Stem Cells. *Methods Mol. Biol.* **2023**, *2593*, 83–92. [[CrossRef](#)]
51. Bhatia, J.K.; Chaudhary, T.; Boruah, D.; Bharadwaj, R. Study of angiogenesis in invasive breast carcinoma by morphometry and immunohistochemistry. *Med. J. Armed Forces India* **2022**, *78*, 345–354. [[CrossRef](#)]
52. Bujor, I.S.; Cioca, A.; Ceaușu, R.A.; Veaceslav, F.; Nica, C.; Cîmpean, A.M.; Raica, M. Evaluation of Vascular Proliferation in Molecular Subtypes of Breast Cancer. *In Vivo* **2018**, *32*, 79–83. [[CrossRef](#)]
53. D'Alfonso, T.M.; Subramaniam, S.; Ginter, P.S.; Mosquera, J.M.; Croyle, J.; Liu, Y.F.; Rubin, M.A.; Shin, S.J. Characterization of CD34-deficient myofibroblastomas of the breast. *Breast J.* **2018**, *24*, 55–61. [[CrossRef](#)]
54. Schulze, A.B.; Schmidt, L.H.; Heitkötter, B.; Huss, S.; Mohr, M.; Marra, A.; Hillejan, L.; Görlich, D.; Barth, P.J.; Rehkämper, J.; et al. Prognostic impact of CD34 and SMA in cancer-associated fibroblasts in stage I-III NSCLC. *Thorac. Cancer* **2020**, *11*, 120–129. [[CrossRef](#)]
55. Barth, P.J.; Ebrahimsade, S.; Hellinger, A.; Moll, R.; Ramaswamy, A. CD34<sup>+</sup> fibrocytes in neoplastic and inflammatory pancreatic lesions. *Virchows Arch.* **2002**, *440*, 128–133. [[CrossRef](#)]
56. Horn, L.C.; Schreiter, C.; Canzler, A.; Leonhardt, K.; Einkenkel, J.; Hentschel, B. CD34(low) and SMA(high) represent stromal signature in uterine cervical cancer and are markers for peritumoral stromal remodeling. *Ann. Diagn. Pathol.* **2013**, *17*, 531–535. [[CrossRef](#)]
57. Vathiotis, I.A.; Moutafi, M.K.; Divakar, P.; Aung, T.N.; Qing, T.; Fernandez, A.; Yaghoobi, V.; El-Abed, S.; Wang, Y.; Guillaume, S.; et al. Alpha-smooth Muscle Actin Expression in the Stroma Predicts Resistance to Trastuzumab in Patients with Early-stage HER2-positive Breast Cancer. *Clin. Cancer Res.* **2021**, *27*, 6156–6163. [[CrossRef](#)]
58. Nguyen, M.; De Ninno, A.; Mencattini, A.; Mermet-Meillon, F.; Fornabaio, G.; Evans, S.S.; Cossutta, M.; Khira, Y.; Han, W.; Sirven, P.; et al. Dissecting Effects of Anti-cancer Drugs and Cancer-Associated Fibroblasts by On-Chip Reconstitution of Immunocompetent Tumor Microenvironments. *Cell Rep.* **2018**, *25*, 3884–3893.e3. [[CrossRef](#)]
59. Ishii, G.; Ishii, T. Review of cancer-associated fibroblasts and their microenvironment in post-chemotherapy recurrence. *Hum. Cell* **2020**, *33*, 938–945. [[CrossRef](#)]
60. San Martin, R.; Barron, D.A.; Tuxhorn, J.A.; Ressler, S.J.; Hayward, S.W.; Shen, X.; Laucirica, R.; Wheeler, T.M.; Gutierrez, C.; Ayala, G.E.; et al. Recruitment of CD34<sup>+</sup> fibroblasts in tumor-associated reactive stroma: The reactive microvasculature hypothesis. *Am. J. Pathol.* **2014**, *184*, 1860–1870. [[CrossRef](#)]
61. Wu, S.Z.; Roden, D.L.; Wang, C.; Holliday, H.; Harvey, K.; Cazet, A.S.; Murphy, K.J.; Pereira, B.; Al-Eryani, G.; Bartonicek, N.; et al. Stromal cell diversity associated with immune evasion in human triple-negative breast cancer. *EMBO J.* **2020**, *39*, e104063. [[CrossRef](#)]
62. Yamashita, M.; Ogawa, T.; Zhang, X.; Hanamura, N.; Kashikura, Y.; Takamura, M.; Yoneda, M.; Shiraishi, T. Role of stromal myofibroblasts in invasive breast cancer: Stromal expression of alpha-smooth muscle actin correlates with worse clinical outcome. *Breast Cancer* **2012**, *19*, 170–176. [[CrossRef](#)]
63. Catteau, X.; Simon, P.; Noël, J.C. Myofibroblastic stromal reaction and lymph node status in invasive breast carcinoma: Possible role of the TGF- $\beta$ 1/TGF- $\beta$ R1 pathway. *BMC Cancer* **2014**, *14*, 499. [[CrossRef](#)] [[PubMed](#)]
64. Akanda, M.R.; Ahn, E.J.; Kim, Y.J.; Salam, S.M.A.; Noh, M.G.; Kim, S.S.; Jung, T.Y.; Kim, I.Y.; Kim, C.H.; Lee, K.H.; et al. Different Expression and Clinical Implications of Cancer-Associated Fibroblast (CAF) Markers in Brain Metastases. *J. Cancer* **2023**, *14*, 464–479. [[CrossRef](#)]
65. Kennel, K.B.; Bozlar, M.; De Valk, A.F.; Greten, F.R. Cancer-Associated Fibroblasts in Inflammation and Antitumor Immunity. *Clin. Cancer Res.* **2023**, *29*, 1009–1016. [[CrossRef](#)] [[PubMed](#)]

66. Toullec, A.; Gerald, D.; Despouy, G.; Bourachot, B.; Cardon, M.; Lefort, S.; Richardson, M.; Rigai, G.; Parrini, M.C.; Lucchesi, C.; et al. Oxidative stress promotes myofibroblast differentiation and tumour spreading. *EMBO Mol. Med.* **2010**, *2*, 211–230. [[CrossRef](#)] [[PubMed](#)]
67. Benyahia, Z.; Dussault, N.; Cayol, M.; Sigaud, R.; Berenguer-Daizé, C.; Delfino, C.; Tounsi, A.; Garcia, S.; Martin, P.M.; Mabrouk, K.; et al. Stromal fibroblasts present in breast carcinomas promote tumor growth and angiogenesis through adrenomedullin secretion. *Oncotarget* **2017**, *8*, 15744–15762. [[CrossRef](#)]
68. Costa, A.; Kieffer, Y.; Scholer-Dahirel, A.; Pelon, F.; Bourachot, B.; Cardon, M.; Sirven, P.; Magagna, I.; Fuhrmann, L.; Bernard, C.; et al. Fibroblast Heterogeneity and Immunosuppressive Environment in Human Breast Cancer. *Cancer Cell* **2018**, *33*, 463–479. [[CrossRef](#)]
69. Germain, C.; Devi-Marulkar, P.; Knockaert, S.; Biton, J.; Kaplon, H.; Letaïef, L.; Goc, J.; Seguin-Givelet, A.; Gossot, D.; Girard, N.; et al. Tertiary Lymphoid Structure-B Cells Narrow Regulatory T Cells Impact in Lung Cancer Patients. *Front. Immunol.* **2021**, *12*, 626776. [[CrossRef](#)]
70. Bonneau, C.; Eliès, A.; Kieffer, Y.; Bourachot, B.; Ladoire, S.; Pelon, F.; Hequet, D.; Guinebretière, J.M.; Blanchet, C.; Vincent-Salomon, A.; et al. A subset of activated fibroblasts is associated with distant relapse in early luminal breast cancer. *Breast Cancer Res.* **2020**, *22*, 76. [[CrossRef](#)]
71. Kieffer, Y.; Hocine, H.R.; Gentric, G.; Pelon, F.; Bernard, C.; Bourachot, B.; Lameiras, S.; Albergante, L.; Bonneau, C.; Guyard, A.; et al. Single-Cell Analysis Reveals Fibroblast Clusters Linked to Immunotherapy Resistance in Cancer. *Cancer Discov.* **2020**, *10*, 1330–1351. [[CrossRef](#)]
72. Barb, A.C.; Pasca Fenesan, M.; Pirtea, M.; Margan, M.M.; Tomescu, L.; Melnic, E.; Cimpean, A.M. Tertiary Lymphoid Structures (TLSs) and Stromal Blood Vessels Have Significant and Heterogeneous Impact on Recurrence, Lymphovascular and Perineural Invasion amongst Breast Cancer Molecular Subtypes. *Cells* **2023**, *12*, 1176. [[CrossRef](#)]
73. Available online: <https://pubmed.ncbi.nlm.nih.gov/?term=CD34%20%2C%20smooth%20muscle%20actin%20breast%20cancer> (accessed on 6 May 2023).
74. Agrawal, S.; Fritchie, K.J.; Fernandez, A.P.; Ko, J.S.; Bergfeld, W.; Rubin, B.P.; Billings, S.D. The capillary lobule variant of radiation-associated angiosarcoma in the setting of breast cancer: A diagnostic pitfall. *J. Cutan. Pathol.* **2023**, *50*, 140–146. [[CrossRef](#)]
75. Strait, A.M.; Bridge, J.A.; Iafrate, A.J.; Li, M.M.; Xu, F.; Tsongalis, G.J.; Linos, K. Mammary-type Myofibroblastoma with Leiomyomatous Differentiation: A Rare Variant with Potential Pitfalls. *Int. J. Surg. Pathol.* **2022**, *30*, 200–206. [[CrossRef](#)]
76. Zhao, L.; Komforti, M.K.; Dawson, A.; Rowe, J.J. Periductal Stromal Tumor of the Breast: One Institution’s Review of 6 Tumors Over a 22 Year Period with Immunohistochemical Analysis. *Int. J. Surg. Pathol.* **2022**, *30*, 370–377. [[CrossRef](#)]
77. Neuzillet, C.; Nicolle, R.; Raffenne, J.; Tijeras-Raballand, A.; Brunel, A.; Astorgues-Xerri, L.; Vacher, S.; Arbateraz, F.; Fanjul, M.; Hilmi, M.; et al. Periostin- and podoplanin-positive cancer-associated fibroblast subtypes cooperate to shape the inflamed tumor microenvironment in aggressive pancreatic adenocarcinoma. *J. Pathol.* **2022**, *258*, 408–425. [[CrossRef](#)]
78. Zhao, Z.; Li, T.; Yuan, Y.; Zhu, Y. What is new in cancer-associated fibroblast biomarkers? *Cell Commun. Signal.* **2023**, *21*, 96. [[CrossRef](#)]
79. Saw, P.E.; Chen, J.; Song, E. Targeting CAFs to overcome anticancer therapeutic resistance. *Trends Cancer* **2022**, *8*, 527–555. [[CrossRef](#)]
80. Du, R.; Zhang, X.; Lu, X.; Ma, X.; Guo, X.; Shi, C.; Ren, X.; Ma, X.; He, Y.; Gao, Y.; et al. PDPN positive CAFs contribute to HER2 positive breast cancer resistance to trastuzumab by inhibiting antibody-dependent NK cell-mediated cytotoxicity. *Drug Resist. Updates* **2023**, *68*, 100947. [[CrossRef](#)]
81. Kato, T.; Furusawa, A.; Okada, R.; Inagaki, F.; Wakiyama, H.; Furumoto, H.; Fukushima, H.; Okuyama, S.; Choyke, P.L.; Kobayashi, H. Near-Infrared Photoimmunotherapy Targeting Podoplanin-Expressing Cancer Cells and Cancer-Associated Fibroblasts. *Mol. Cancer Ther.* **2023**, *22*, 75–88. [[CrossRef](#)]

**Disclaimer/Publisher’s Note:** The statements, opinions and data contained in all publications are solely those of the individual author(s) and contributor(s) and not of MDPI and/or the editor(s). MDPI and/or the editor(s) disclaim responsibility for any injury to people or property resulting from any ideas, methods, instructions or products referred to in the content.